LODZ UNIVERSITY OF TECHNOLOGY
Faculty of Electrical, Electronic, Computer and Control Engineering

Master of Engineering Thesis

Investigation into power electronic converters technologies to improve system performance for future aircraft electrical power systems

Badania technologii elektronicznych przetwornic mocy w celu poprawy osiągów w układach elektrycznych samolotów przyszłości

Daniel Dobiński

Student's number: 208253

Supervisors:
Krzysztof Tomalczyk, PhD
Patrick Norman, PhD

Łódź, 2017

Abstract

The purpose of this project is to investigate the power electronic block which is the link between the electrical grid and the motors for future propulsion system, fulfilling all the rigid requirements of aircraft industry e.g. very high efficiency, possible small weight and volume, high power, and reliability, with an emphasis on the impact of the modulation techniques on the system performance

It consists of design and simulation of a system of 2 *MVA* based on a three phase bidirectional AC/DC, Voltage Source Converter for propulsion applications, with nominal voltage of 1000 *V* (DC bus) and frequency of 600 *Hz* and investigation of its properties (losses, weight, volume, power quality) to determine possible challenges of real implementation. The simulations consists of two types: the three phase inverter and three-phase converter together with various modulation techniques. The converters were modelled with a resistive load, however, one additional simulation shows the possibility of implementation of the inverter together with a model of an induction machine and test of its capabilities, such as maintaining its speed and good transient behavior under various load condition.

Most of the project success criteria were achieved. Two models of the three phase rectifier and the three phase inverter were designed and simulated. Various modulation techniques were tested together with other system parameters like: filters cut-off frequency and operating frequency. Additional model of the induction machine was confirmed to work properly and its efficiency and draft of harmonic analysis were shown. MEA (More Electric Aircraft) is quite new research topic, especially when attempting totally exchange petrol engines for electrical machines, there is still much work to be done in this area, however, thesis gives a glimpse into the issue.

1

Streszczenie

Celem niniejszego projektu jest zbadanie bloku elektroniki mocy, który łączy sieć elektryczną z system napędowym, jednocześnie mając na uwadze ścisłe wymagania przemysłu lotniczego takie jak: wysoka sprawność, możliwie mała waga i objętość, duża moc, wysoka niezawodność; ze szczególnym naciskiem na wpływ różnego rodzaju modulacji na wyniki systemu.

Praca składa się z zaprojektowaniu oraz symulacji systemu o bazowej mocy 2 *MVA*, opartym na trzyfazowym, dwukierunkowym przetworniku mocy AC/DC, stałonapięciowym dla napędów lotniczych z nominalnym napięciem 1000 *V* (bus DC) i częstotliwością 600 *Hz*. Celem projektu jest zbadanie właściwości systemu (objętość, waga, sprawność, jakość mocy) oraz analiza ewentualnych problemów przy implementacji. Projekt składa się z dwóch rodzajów symulacji, trzyfazowego prostownika oraz trzyfazowego falownika z zastosowaniem różnego rodzaju modulacji. Przetworniki były zaprojektowane z użyciem obciążenia rezystancyjnego, ale została również dodana dodatkowa symulacja która ukazuje możliwość zamodelowania obciążenia jako silnik indukcyjny oraz przetestowaniu jego możliwości takich jak podtrzymanie zadanej wartości prędkości czy zachowanie w stanach dynamicznych w różnych warunkach obciążenia.

Projekt został zakończony pomyślnie, spełniając większość z początkowych kryteriów. Dwa modele symulacyjne zostały zaprojektowane oraz przetestowane wraz z różnymi technikami modulacji oraz innymi parametrami takimi jak częstotliwość odcięcia filtrów czy częstotliwość przełączania. Dodatkowy model z silnikiem indukcyjnym został zasymulowany dając poprawne wyniki w stanach dynamicznych. Jego sprawność oraz wstępna analiza Fouriera jednej z faz prądów statora zostały zaprezentowane. Temat MEA (More Electric Aircraft) jest dosyć nowy, szczególnie całkowita próba zamiany silników odrzutowych przez elektryczne, jest jeszcze wiele do zrobienia w tej dziedzinie, jednak praca magisterska daje możliwość rozeznania w ewentualnym wprowadzeniu tego rodzaju technologii.

Table of Contents

4

1. Introduction

1.1. Motivation

The increasingly growing need for electric energy and the extended emphasis on environmental protection made the efficiency issue very important. These targets refer to the projected 20 % improvement in energy efficiency by 2020 from the "Action Plan for Energy Efficiency: Realizing the Potential" set out in 2009 by European Parliament and of The Council European Union [1]. The Advisory Council for Aeronautics Research in Europe has also set goals to be achieved by 2020 for air transportation. Among these are:

- A 50% reduction of carbon dioxide emissions.

- An 80% reduction of nitrogen oxide emissions.

- An 50% reduction of external noise, maintenance, and disposal product life cycle [14].
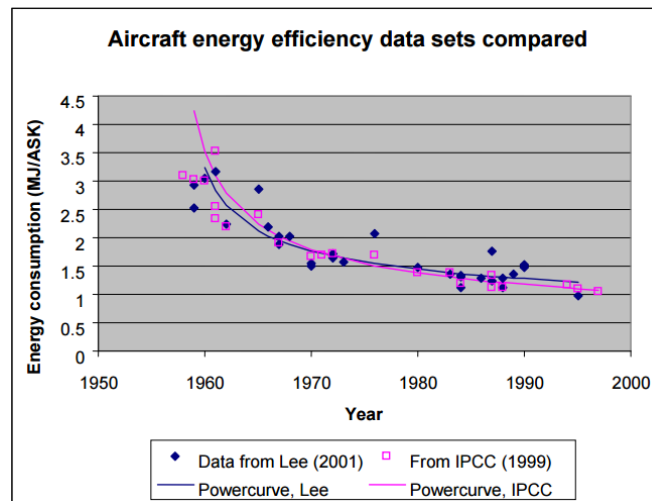
Fig. 1. Aircraft energy efficiency data sets compared [15].

Efficiency of the traditional aircraft is increasing every year, and many studies presented a constant annual percentage efficiency gain of 1.2% and 2.2% a year in the future. Unfortunately, even if the efficiency is nearly 100%, aircraft will still burn considerable amounts of fuel, resulting in contamination of the environment. Moreover, the rate of increase of efficiency is getting smaller [15]. For that reason, recent trend in the research is to exchange petrol engines for electric motors.
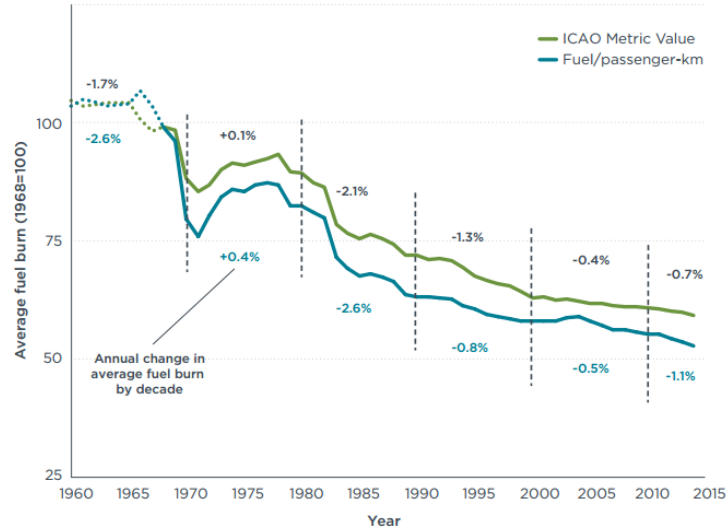
Fig. 2. Average fuel burn for new commercial jet aircraft, 1960 to 2014 [17].
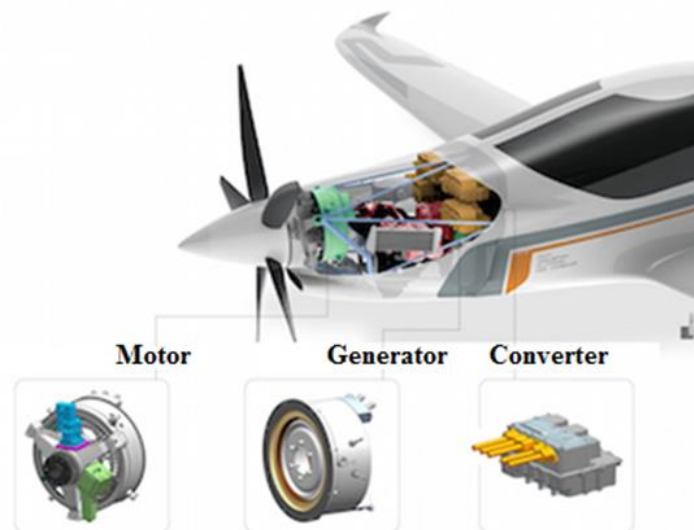
1.2. Aim

Fig. 3. Future power propulsion system [18].

Typically, an airplane is equipped with a DC battery and a generator that can supply motors or the rest of electronic DC devices available on board (lights, monitors, compressors etc.) In the future, the propulsion system itself is planned to also be supplied from the electrical system available on the plane. The goal of this project is to investigate the power electronic block power which is the link between the electrical grid and the motors for future propulsion system, fulfilling all the rigid requirements of aircraft industry e.g. very high efficiency, possible small weight and volume, high power, and reliability, with an emphasis on the impact of the modulation techniques on the system performance.

1.3. Objectives
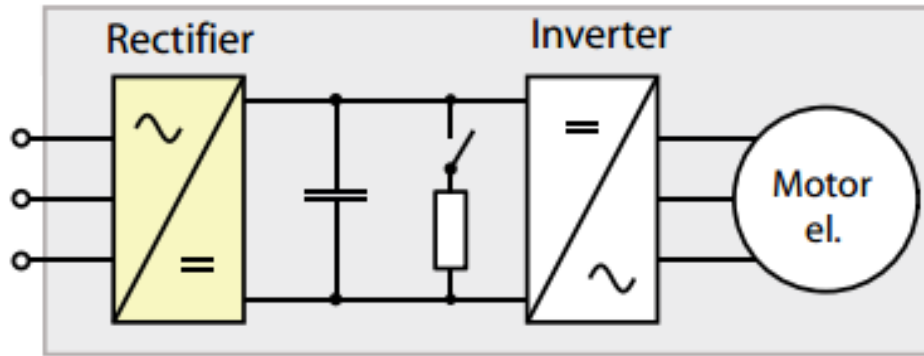
Fig. 4. Power electronic block [19].

The objective of this project is to design and simulate a system of 2 MVA based on a three phase bidirectional AC/DC, Voltage Source Converter for propulsion applications, with nominal voltage of 1000 V (DC bus) and frequency of 600 Hz and to also study its properties (losses, weight, volume, power quality) to determine possible challenges of real implementation. The simulations consists of at two types: the three phase inverter and three-phase converter together with various modulation techniques.

1.4. Technology overview

Many aircraft manufacturers are planning to develop future aircraft propulsion systems in such a way that they will be hybrid or entirely based on electricity. Among these are:
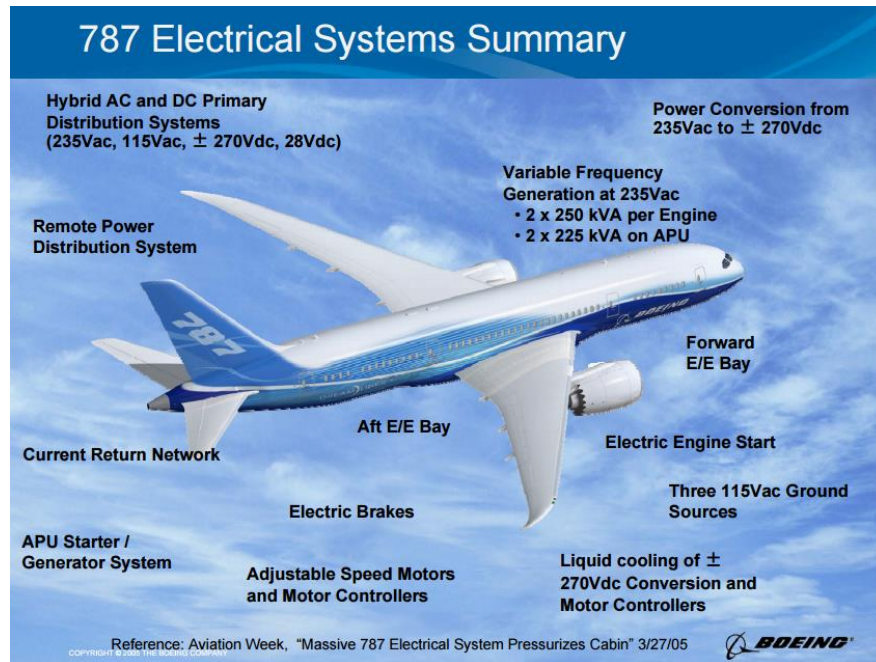
"Theory and tools for trade-off studies:

ETH Zürich, TU Darmstadt, E.on - RWTH Aachen, Univ. Strathclyde, KIT, BHL

Experiences from Business Fields:

Airbus, Siemens, Alstom, General Electric, Rolls Royce, Safran, Infineon"**[2].**

Fig. 5. Future power propulsion system [16].

An example of electrification of airplanes is Boeing 787 *'Dreamliner'*. It is the first commercial airplane to have a 230 variable frequency distribution system, and an electrically powered air conditioning system. It is also the first airplane to utilize electro-mechanical flight control actuators [16].

Fig. 6. Siemens electric aircraft maiden flight [18].

Siemens researchers have developed a new type of electric motor that, powered an Extra 330LE aerobatic airplane and made its maiden flight on June 24th 2016. Motor of 50 kilograms, delivers a continuous output of about 260 kW. This advance means that hybrid-electric aircraft with four or more seats will now be possible. According to Siemens, electric

drives are scalable. Siemens and Airbus will be using the record-setting motor as a basis for developing hybrid-electric propulsion systems with an expectation of constructing an aircraft with up to 100 passengers and a range of 1000 km by the end of 2030 **[18]**.

2. Theoretical background

2.1. Digressions, about the DC busbar

One could argue that the double conversion from AC to DC and then from AC to DC in not necessary due to the fact that both generator and motor are AC type. The reason for doing it, is lack of AC controllable devices. The only AC device that one dispose of is the transformer, but it has no additional input capable of controlling the currents and voltages needed in order to appropriately control the motor torque and speed. There are other ways to control the aero plane speed, keeping the propellers' rotational speed constant: changing their angle of attack, or slightly changing the frequency of the AC generator (no abrupt changes are allowed), however, these types of design do not concern this particular project, and there is no unanimous opinion, which concept performs better.

2.2. Generator

Permanent Magnet Synchronous Machines (PMSM) and Switched Reluctance Machines (SRM) are promising generator technologies thanks to high power density, robustness and temperature tolerance **[22]**. The generator may be used as starter motor which can reduce the weight of the aircraft **[23]**.

2.3. Overview of switches

Power electronics comprises of switches of many types and parameters. One can divide them into 3 groups:

- Diodes (not controllable).
- Thyristors (turned on by a control signal, but turned off by the power circuit).
- Controllable switches e.g. MOSFET/IGBT (fully controllable by control signal) **[4].**

Unfortunately switches have their limitations, the most significant are:

- Maximal breakdown voltages.
- On state resistance.
- Maximal switching frequency.

- Power dissipation capability **[3]**.

There is no available electron device that would simultaneously provide high correlation with the ideal switch. Every device has its advantages and disadvantages, the process of selection requires a tradeoff between various parameters. For example it is impossible to have high breakdown voltage and low on state resistance at the same time.
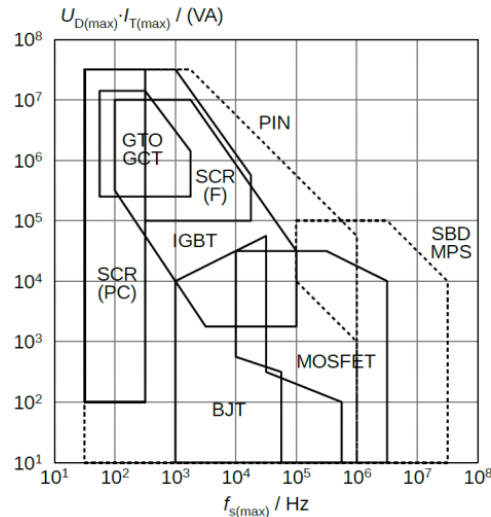

Fig 7. Parameters of available electron devices, Power=f(Swiching frequency) [4].

Recently the widely used switches are IGBT (Insulated Gate Bipolar Transistor) which have very high power dissipation capability, as well as MOSFET (Metal-Oxide Semiconductor Field-Effect Transistor) which provides relatively high switching frequency.

For most of the power electronic devices silicon is the only semiconductor material used; however there are other materials of intense interest such as Silicon Carbide. SiC has a significantly larger energy gap to silicon, therefore, the switches made of that material can withstand higher breakdown voltage. There are many SiC MOSFET switches available now in the market.

2.4. Rectifier and Inverter

Rectifier is an electron device capable of converting the AC power into DC power, inversely an inverter is a device that converts AC power into DC power. Both of the concepts are thoroughly described in the literature e.g. **[3]**.
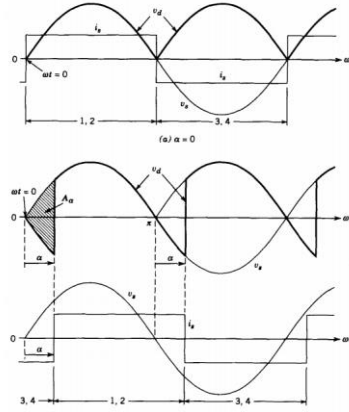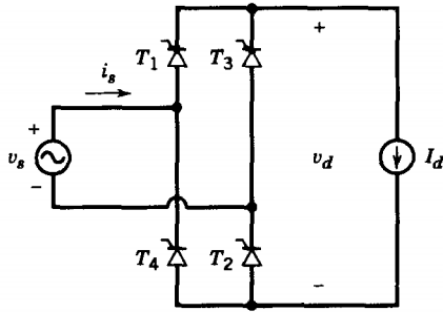
Fig 8. Phase rectifier topology [3].   Fig 9. phase rectifier waveform [3].
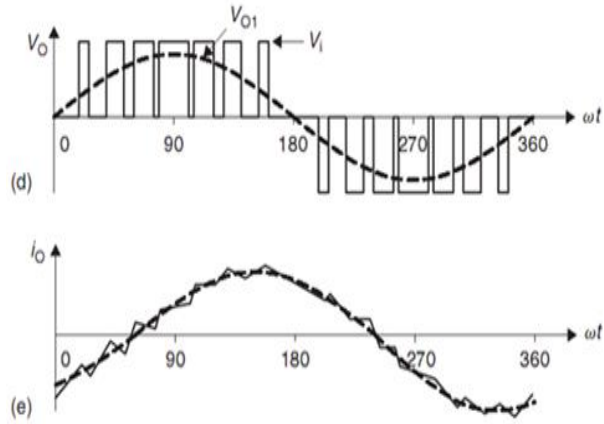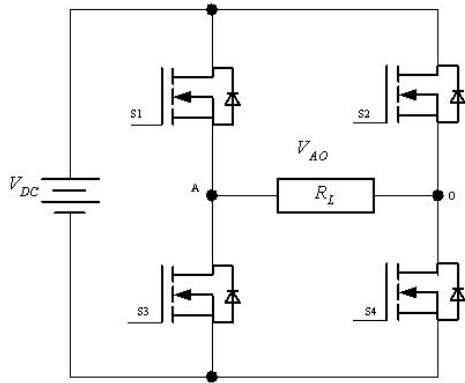

Fig. 10. Phase inverter topology [5].   Fig. 11. phase inverter waveform [6].

Figures presented above depict one phase rectifier and an inverter waveforms of the basic operation. We can see how the power is conversed from AC to DC and vice versa. The topology of both devices is quite similar and it is possible to create bi-directional converter using full bridge configuration. The additional part that is not presented above are filters as well as block of control of switches.

2.5.   Filters

A filter is a device that passes electric signals at certain frequency ranges while preventing the passage of others. The most common type of filters is a low pass filter. It passes the low frequencies and attenuates the high frequency signals starting from a particular frequency, called the cut-off frequency. Unfortunately, ideal filters do not exist, and if they did, they would eliminate signals above the cut-off frequency and perfectly pass signals below.

11

Therefore, the cut-off frequency is defined as the frequency where output power has dropped to half.
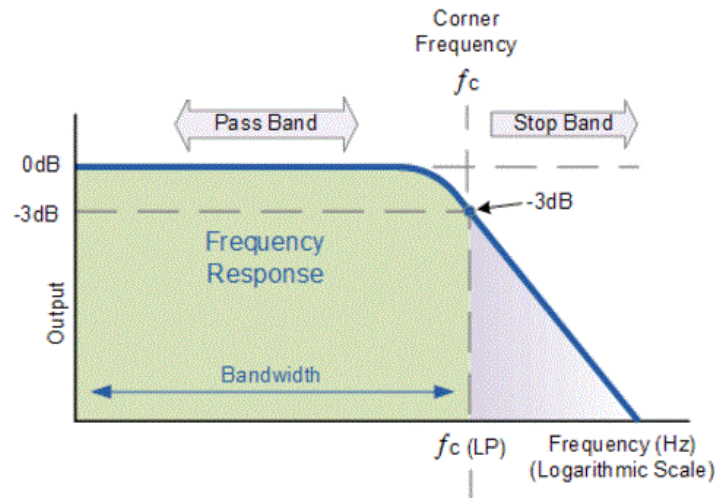
Fig. 12. Frequency response of low-pass filter [7].

There are a vast number of possible filters types and implementations. The most common difference is the presence of opamp (operational amplifier), which is an active filter, versus topologies that consist of only passive components, such as inductors, resistors, and capacitors. Another common division is the filter order, which is linked to the shape of the filter frequency response **[8]**. Due to high power, it is not possible to use active filters for power systems. The only reasonable solution is usage of passive filters.

2.6. PWM

PWM (Pulse-width modulation) is a modulation technique used in many applications, e.g. encoding of transmission or control. The only two possible states are "high" and "low" or sometimes "negative high". The amount of delivered power is controlled by regulating the time when the signal is on and off. The fraction of one period in which a signal or system is active is called duty cycle and it is expressed as the percentage of being fully on (100%) **[10].** An inverter can produce only 3 states of the voltage as well. It could keep the duty cycle constant, but then the output waveform would contain a high value of undesirable harmonics that has to be filtered later on. In order to reduce the size of filter elements, it is better to provide an input signal for a filter that is already of a better quality. That is why duty cycle must be changing throughout the period. There is still room for choice of the modulation, bipolar PWM or unipolar PWM.
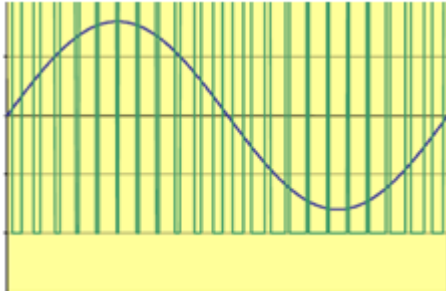
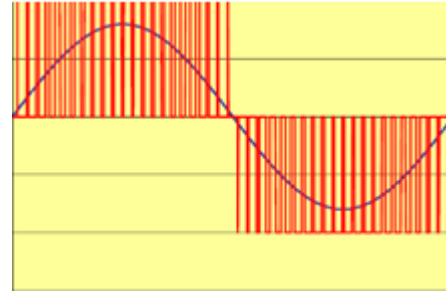*Fig. 13. Bipolar PWM [11]*   *Fig. 14. Unipolar PWM [11]*

Bipolar PWM consists of only 2 levels, $-V_{dc}$ and V_{dc}, whereas in unipolar PWM zero voltage state is also present. Fourier analysis confirms that unipolar PWM outperforms bipolar when it comes to THD quality. However, a zero state gives a chance to the flow of the leakage current **[10].**

2.7.   Rigid requirements for the aircraft industry

As mentioned in the *section 1.1. Motivation*, the demand to optimize aircraft performance is growing. The concept under the name of MEA (More Electric Aircraft) provides ideas for the utilization of electric power for non-propulsive systems, as well as all electric aircraft. The optimization considers a decrease of maintenance cost, reduction of gas emissions and fuel consumption and increase of reliability **[12]**. For that particular project, those factors translate into key parameters of the electrical converters, due to the fact that bi-directional AC/DC converter for propulsion applications is taken into consideration.

2.7.1.   Efficiency

The fuel consumption may decrease as long as high efficiency is kept. Besides the loss of the generator and motor, there are two types of losses in power electronic block:

Steady state losses depends on state resistance of the switches. They may be minimized, however, it is impossible to produce a switch that would have a small voltage drop and high power capability.

Transient losses are created at the time of the turning off and on of the device. They depend on the curves of the current and voltages during that time. They may be diminished if the turning off/on time is minimized. That feature is linked to the parameter called maximal switching frequency.
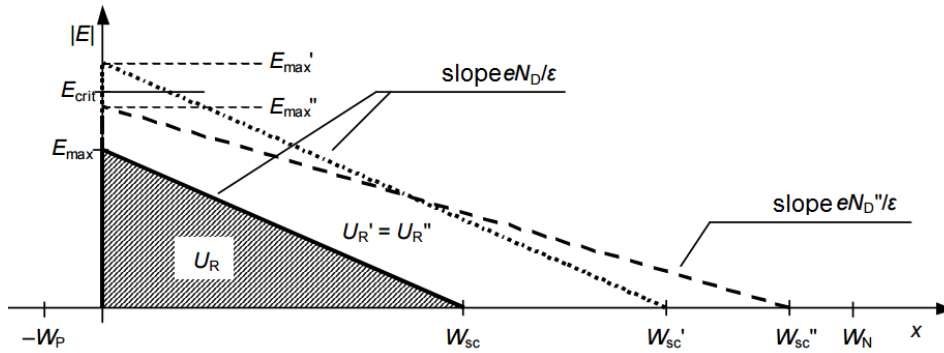
2.7.2. Power capability and Volume

Fig. 15. Distribution of electrical field for PN junction, for different semiconductor doping and applied voltage [4].

Maximal voltage breakdown can be characterized by value of the field in the PN junction (the field has the maximal value in that point). It can be estimated by following equation:

$$U_r = \frac{1}{2}W_{sc}E_{max} = \frac{1}{2}\frac{E_{max}}{\frac{eN_d}{\varepsilon}}E_{max} = \frac{\varepsilon E_{max}^2}{2eN_d} \tag{2.1.}$$

U_r - Breakdown voltage

e - Electron charge

N_d - Semiconductor doping

W_{sc} - Width of the depletion region

E_{max} - Maximal electric field

In order to increase the breakdown voltage, two simultaneous changes are needed, decrease of the semiconductor doping and increase of the width of the depletion region. The maximal current also depends on the volume of the device, the higher the volume is the higher current flow is possible without damaging the switch. In order to analyze the exact impact of both parameters it is needed to analyze the exact internal structure of any switch, however one can conclude that the power capability is proportional to volume of power converter.

2.7.3. Reliability and cooling

Thermal instability is a local problem of the structure because the thermal distribution is heterogeneous, moreover thermal runaway has the characteristics of the positive feedback. When the temperature of a particular area increases, the resistivity decreases causing the current crowding and hot spots are created. Thermal breakdown can be caused by various

14

reasons and it irreversibly damages the device, that is why it is crucial to operate in SOA (Safe Operation Area), and to apply appropriate cooling, especially when the operating power is assumed to be high. Unfortunately, an effective cooling system takes space and it is an added weight, which is undesirable for the aircraft industry.

2.8. Aircraft standard

Converter has to comply with aircraft standards, primarily the airborne standard DO160F [20] and the military standard MILSTD704F [21]. Companies create also their own standard that may be more stringent.

Limitations:

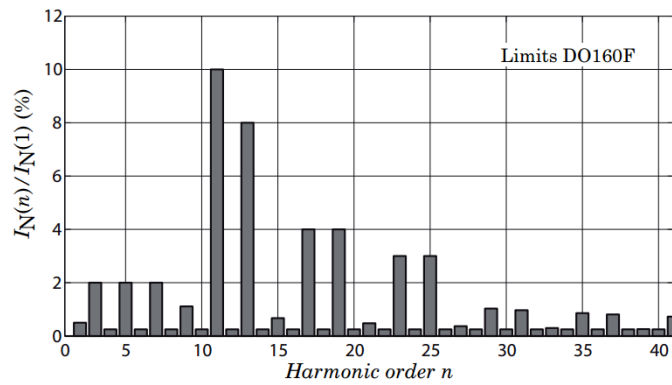### 2.8.1. Individual current harmonic limits.

Fig. 16. Individual current harmonic listed in standard D0160F [19].

2.8.2. Power factor

The power factor of AC interface is limited to 0.85 lagging and 1 for power levels greater than 50 % of the rated output power. In the standard MIL-STD407F [21] a leading power factor is not allowed for equipment with output power levels greater than 500 VA to prevent self-excitation of synchronous generator. It is not specified, whether this limitation also apply to transients. This limitation has to be considered due to the need of the design of EMI filter [19].

2.9. Bidirectional vs Unidirectional converter.

Bidirectional active rectifier systems, have a great capability of controlling the reactive power, also at no load condition, which is only possible to a limited extend for an unidirectional rectifier. Drawbacks are reduced reliability due to possible shoot-through of a bridge leg resulting in a short circuit of the DC-voltage, the high current stress on the

semiconductors and the involvement of the MOSFET body diode causing a substantial limitation of the switching frequency.

2.10. VLBBC (Voltage Link Back-to-Back connected Converter) vs MC (Matrix Converter)

MC is more efficient and shows a volume reduction (by factor of 1.5 for the system reported in **[25]**) of the passive components including heat sink. Unfortunately, the higher achievable power density of MCs is a price for: limited output voltage step-up capability, constrained reactive input power compensation and disability of single-phase operation **[25]**.

2.11. Induction motor
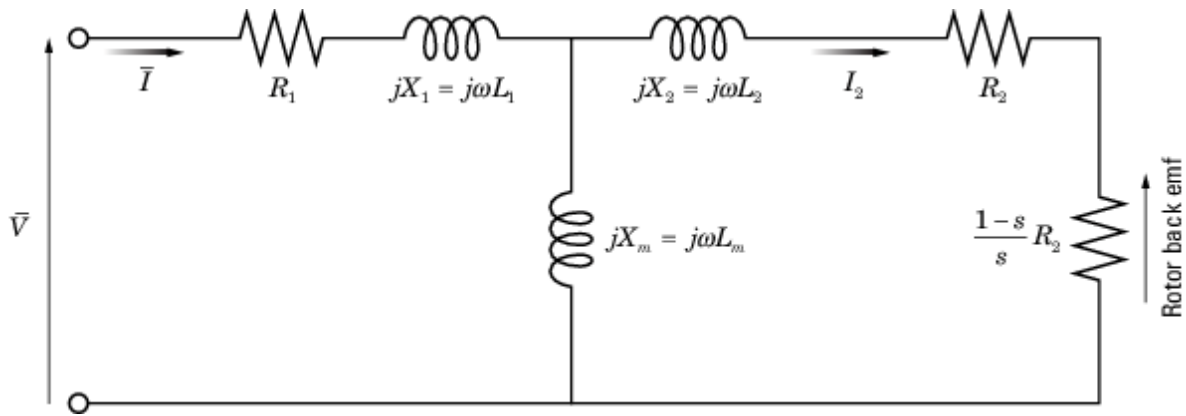
Fig. 17. Equivalent circuit model of the induction motor per phase. [29].

- R_1 is the stator resistance.
- R_2 is the rotor resistance with respect to the stator.
- L_1 is the stator inductance.
- L_2 is the rotor inductance with respect to the stator.
- L_m is magnetizing inductance.
- s is the rotor slip.
- $\bar{V}$ and $\bar{I}$ are the sinusoidal supply voltage and current phasors.

Rotor slip s is defined in terms of the mechanical rotational speed ω_m, the number of pole pairs p, and the electrical supply frequency ω by

$$s = 1 - \frac{p\omega_,}{\omega} \qquad (2.1)$$

This means that the slip is one when starting, and zero when running synchronously with the supply frequency.

16

For an n-phase induction motor the torque-speed relationship is given by:

$$T = \frac{npR_2}{s\omega} \frac{V_{rms}^2}{\left(R_1+R_2+\frac{1-s}{s}R_2\right)^2 + (X_1+X_2)^2} \qquad (2.2) \ [29]$$

1. Simulations

All the simulations were done using the matlab simulink compiling with mfile in order to make calculations and plots automatically. The simulations consist of two types: the three phase inverter and three-phase converter together with various modulation techniques (control). All the simulations based on active rectifier, used IGBT switch with R_{on} equal to 0.0025 Ω.

1.1. Initial Parameters:

It is impossible to predict the exact value of the systems features before designing and simulating it (e.g. V_{dc} will fluctuate), however, initial parameters of the system were set and are treated as a reference values (the actual performance may slightly differ).

AC frequency = 600 Hz

V_{dc}=1000V

$V_{line \ (RMS)}$ = 1223.7V

S= 2 MVA, cos(φ)=1

1.2. Load

Load is a very important part of the design and its value has to be estimated at the early stage of the project in order to meet the power requirement. During this project it was assumed that the load is resistive, however, for real application inductive load should be considered. Phase current and the value of resistor can be calculated using equation 2.1.

$$P = 3I_{phase(RMS)}V_{phase(RMS)}\cos(\varphi) \qquad (3.1)$$

$$I_{phase(RMS)} = \frac{P}{3V_{phase(RMS)}\cos(\varphi)} \qquad (3.2)$$

$$I_{phase(RMS)} = \frac{2*10^6}{3*707.1057*1} = 942.81 \ A \qquad (3.3)$$

$$I_{phase(pp)} = I_{phase(RMS)} * \sqrt{2} = 942.81 * \sqrt{2} = 1333.33 \ A \qquad (3.4)$$

$$R_{load} = \frac{V_{phase \ (pp)}}{I_{phase \ (pp)}} = \frac{1000 \ V}{1333.3 \ A} = 0.75 \ \Omega \qquad (3.5)$$

Having the value of resistance it is possible to apply it in the matlab simulation and then change it, if does not meet systems requirements.

1.3. Inverter
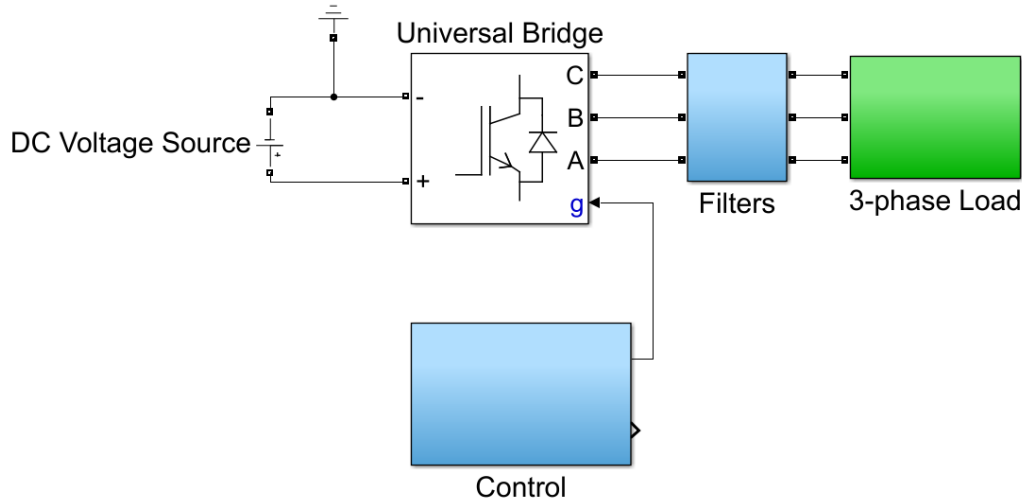
Fig. 18. DC/AC converter, block diagram.

Having set all the values of the block it was possible to implement the inverter. It consists of following blocks: Source, Universal Bridge, Control, Filter, Load.

1.3.1. Filtering
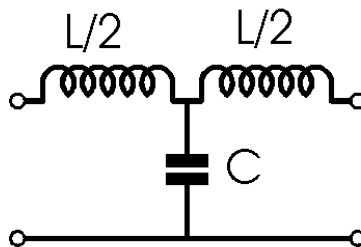
Fig. 19. A Passive 2nd order LC Tee low pass filter topology [13].

A Passive 2nd order LC Tee low pass filter was chosen for inverter output. The elements value were calculated using the equations presented in figure 19**.** The best cut-off frequency was obtained experimentally to provide the best step up capability of the inverter The same type of filters were used for all type of modulations. The values of the inductance and capacitance are 159 µH and 566 µF (cut-off frequency equals to 750 *Hz*).

```
z=0.75;
fcut=[600 750]
N=4; %number of filters
for i=1:N %calculation of C and L for LC Tee filter
    Ltee(i)=z/(2*fcut(i)*3.14);
    Ctee(i)=1/(z*fcut(i)*3.14);
end;
```

Fig. 20. Part of inverter matlab mfile.

1.3.2. SPWM modulation

It was decided to use IGBT with on-state resistance equal to 0.0025 Ω switches and unipolar PWM control with the switching frequency ten times higher than the frequency of the desired output signal.

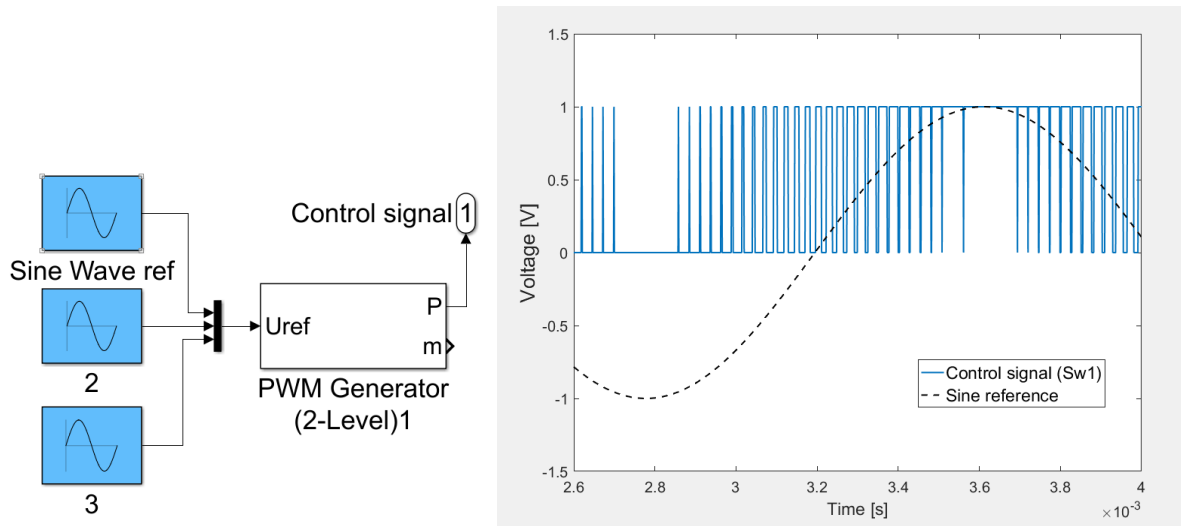### 1.3.2.1. Control

Fig 21. Control and reference voltage of one switch 1.

"The pulses are generated by comparing a triangular carrier waveform to a reference modulating signal and three reference signals are required to generate the pulses for a three-phase, single bridge." **[25]** The shape of the control signal is accurate and in accordance to the theoretical assumptions.
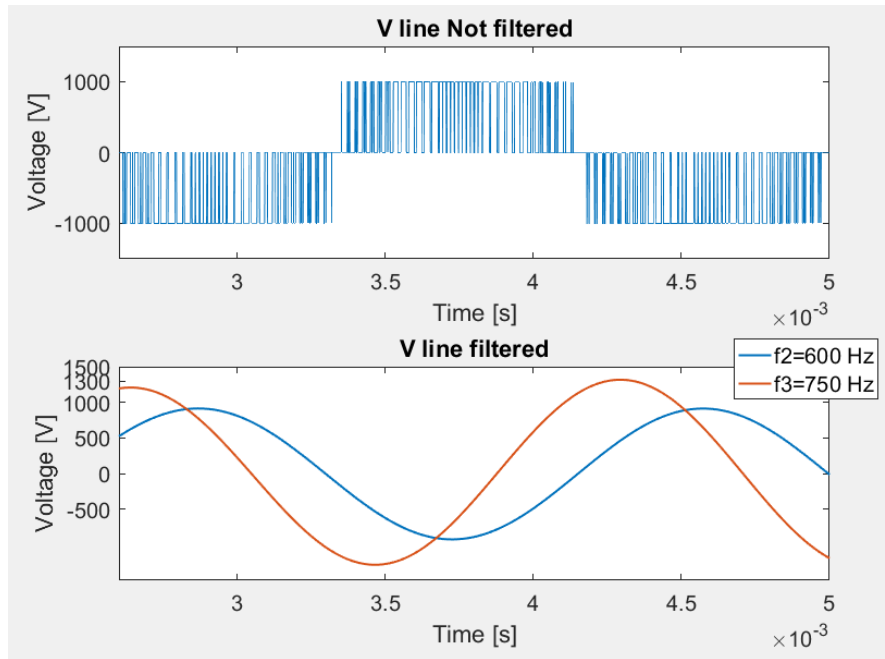
Fig 22. Line voltage (V_{ab})with no filtration [upper], Line voltage (V_{ab}) with filtration [lower].

In the picture above only one line voltage is presented, the shape of both filtered and non-filtered voltages are accurate. One can see a different impact of applying a filter with different value of cut-off frequency. It seems that the optimal cut-off frequency for 2nd order low pass filter is around 750 kHz. It is not a surprise because at the cut-off frequency the power of the signal would already dropped by two. Output power is 60 %   (1.2 *MW*) of the initially designed value. Reactive power is equal to zero after filtration (meets the power factor requirement). In addition to that, a Fourier transform was performed on the not filtered voltage:
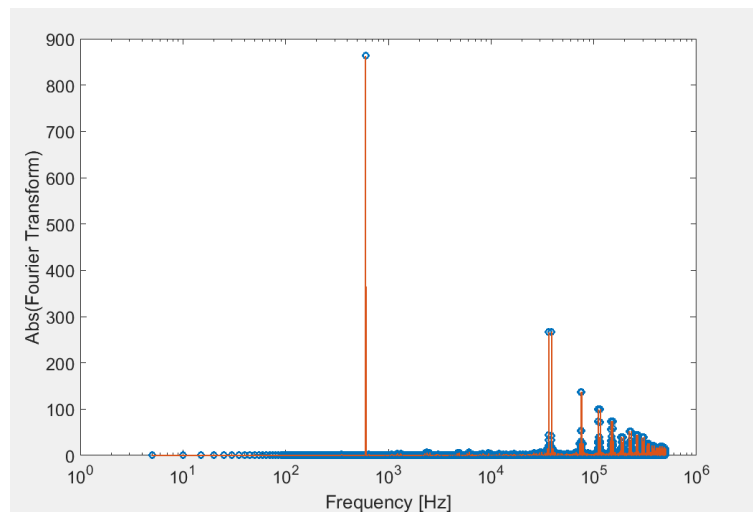
It is clearly seen that the highest harmonic appear at 600 Hz, all the other values are the undesired signal that should be filtered out. Total harmonic distortion factor was calculated using following formula:

$$THD = \frac{\sqrt{\Sigma_{i>1} V_i^2}}{V_1} = 60,95\ \%$$ **(3.6.)**

The result of THD give and idea of how much the filters dimensions could be smaller in reality comparing to the other modulations, however, more testing should be done in order to validate the results. It is worth to mention that the significant amplitudes appeared at the frequencies different than the multiples of the fundamental and were taken into account.
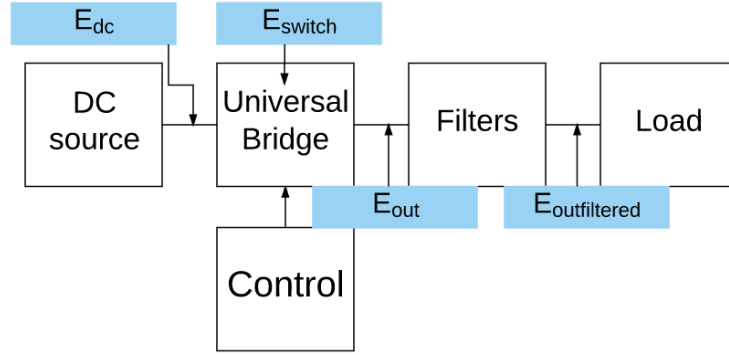

Fig 24. Calculation of efficiency.

The last step was calculating the efficiency of the converter. According to the law of conservation of energy, the input energy (E$_{dc}$) has to be equal to the sum of output energy (E$_{outfiltered}$) and losses. E$_{out}$ should be equal to E$_{outfiltered}$, because the filter is LC type, therefore no resistive losses are present. The ideal case would be calculation of the energy within one period, but due to a shifting properties of the blocks, it is easier to calculate the energy over more than one cycle, having in mind that the result is encumbered with error of one cycle. The energy calculation consisted of a calculation of the power, and integrating it from the start of steady state behavior (time = 0.01 s neglecting the transient) up to the end of the simulation (t = 0.5 s).
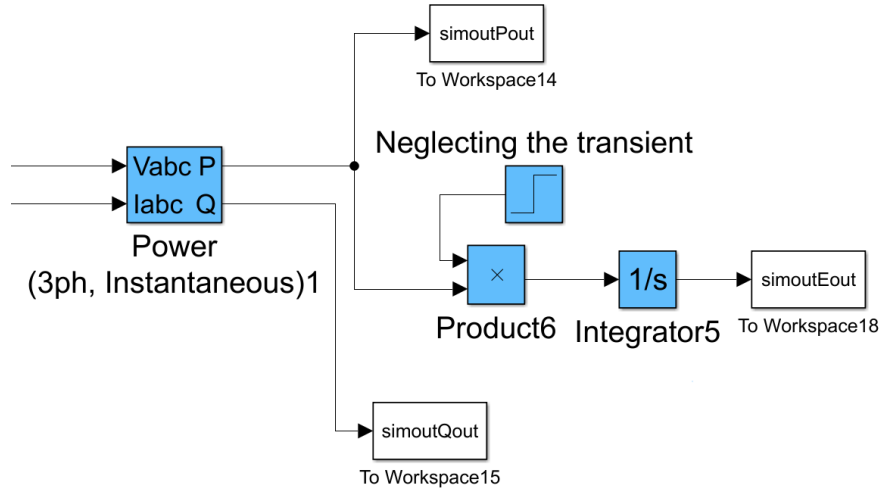
Fig 25. Energy calculation block.

$$N_{cycles} = \frac{t_{steadyState} - t_{simulationEnd}}{Period} = \frac{0.5 - 0.01}{1/600} = 294, \text{ number of periods} \quad (3.7)$$

	E_{dc} [W]	$E_{switch1}$ [W]	E_{out} [W]	$E_{outFiltered}$ [W]
SPWM	594541,6	784,7	587894,6	587905,6

Table 1. Calculation of energy, 294 cycles.

$$\boldsymbol{Efficiency} = \frac{E_{in}}{E_{out}} = \frac{E_{outFiltered}}{E_{dc}} = \frac{587905,6}{594541,6} = \mathbf{98.89}\% \quad (3.8)$$

THD ($V_{not\text{-}filtered}$)	**Losses**	L	C	Power (ref to 2 MW)
60,95 %	**1.11 %**	2x 159 uH	566 uF	60 %

Table 2. Features summary for SPWM modulation, filter with f_{cutoff} = 750 Hz.

1.3.3. SHE modulation

Selective harmonic elimination modulation is based on a signal with such a frequency which would eliminate specific undesired harmonics. The switching angles have to be calculated, which is a considerable computational effort. Despite the fact that its implementation is more complex than SPWM modulation, its output voltage and current have higher quality, the ripple in the DC link is also smaller. It means that smaller filters can be implemented. Switching frequency can be reduced by 2 compared with the conventional SPWM scheme [27].

Fig 26. Generalized output waveform of the single phase inverter (magnitude normalized) [27].
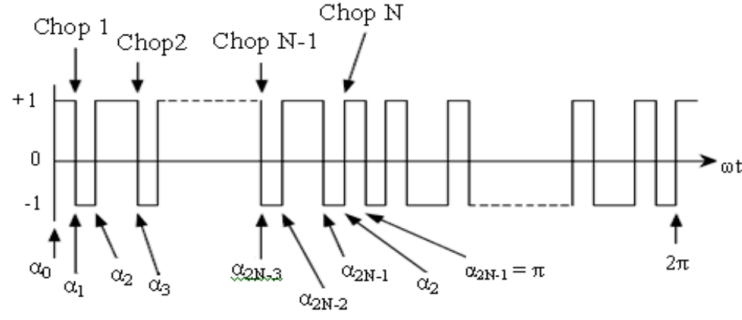
1.3.3.1.   Control

Theoretically elimination of any number of harmonics is possible by chopping a square wave a number of times. It is assumed that the periodic waveform has half-wave symmetry and unit amplitude.

$$-1 + 2\cos\alpha_1 - 2\cos\alpha_2 + 2\cos\alpha_3 - \frac{\pi M}{4} = 0$$

$$\alpha_1 < \alpha_2 < \alpha_3 < \frac{\pi}{2}$$

$$-1 + 2\cos 3\alpha_1 - 2\cos 3\alpha_2 + 2\cos 3\alpha_3 = 0$$

$$-1 + 2\cos 5\alpha_1 - 2\cos 5\alpha_2 + 2\cos 5\alpha_3 = 0$$

Fig 27. Set of equation for harmonic elimination.

The set of equations can be only solved numerically. Seidel's method and Newton's method are popular method in solving this kind of problem. In this project `lsqnonlin()` matlab function was used, which solves nonlinear least-squares curve fitting problems. Because of the fact it is a very complex mathematical problem to eliminate 3rd harmonic, other harmonics were eliminated: 5th,7th 9th 11th ,13th ,15th. Code is available in the appendix.

Table 3. Solutions for N=3, 5 and 7, m=1.

x1 [rad]	x2 [rad]	x3 [rad]	x4 [rad]	x5 [rad]	x6 [rad]	x7 [rad]
0.040294	0.060186	0.095888	0.213319	0.28249	0.483156	0.51038

Table 4. Delay and pulse width.

	Delay [us]	Pulse Width %	Pulse Width [time]
1	10,69	0,32	5,28
2	25,44	1,87	31,15
3	74,93	3,19	53,23
4	135,38	33,75	562,57
5	705,17	3,19	53,23
6	776,75	1,87	31,15
7	817,37	0,32	5,28
8	833,33	0,64	10,69
9	849,30	0,57	9,47
10	889,92	1,10	18,35
11	961,49	0,43	7,22
12	1531,28	0,43	7,22
13	1591,73	1,10	18,35
14	1641,23	0,57	9,47
15	1655,98	0,64	10,69

Table 5. Firing angles.

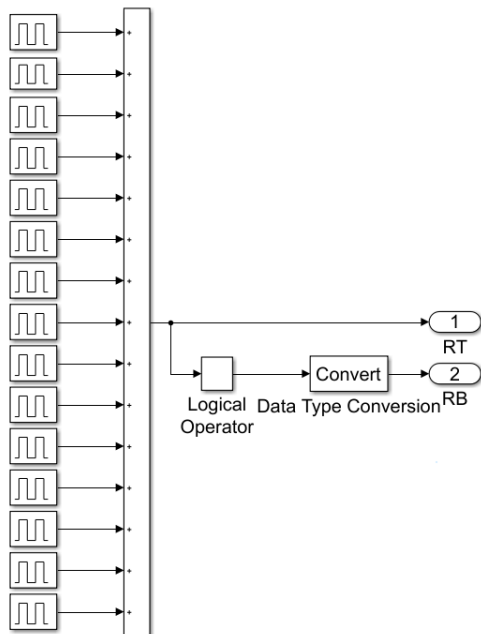| Angle N	[rad]	[degrees]
Alpha1	0,04	2,31
Alpha2	0,06	3,45
Alpha3	0,10	5,49
Alpha4	0,21	12,22
Alpha5	0,28	16,19
Alpha6	0,48	27,68
Alpha7	0,51	29,24
Alpha8	2,63	150,76
Alpha9	2,66	152,32
Alpha10	2,86	163,81
Alpha11	2,93	167,78
Alpha12	3,05	174,51
Alpha13	3,08	176,55
Alpha14	3,10	177,69
Alpha15	3,14	180,00
Alpha16	3,18	182,31
Alpha17	3,20	183,45
Alpha18	3,24	185,49
Alpha19	3,35	192,22
Alpha20	3,42	196,19
Alpha21	3,62	207,68
Alpha22	3,65	209,24
Alpha23	5,77	330,76
Alpha24	5,80	332,32
Alpha25	6,00	343,81
Alpha26	6,07	347,78
Alpha27	6,19	354,51
Alpha28	6,22	356,55
Alpha29	6,24	357,69
Alpha30	6,28	360,00

Fig. 28. Modulation generator block.

Having in mind that all the solutions are the firing angles and that the signal is symmetrical, one can obtain all firing angles and transform that data into delay and pulse width of the matlabs pulse generator blocks.

1.3.3.2. Results
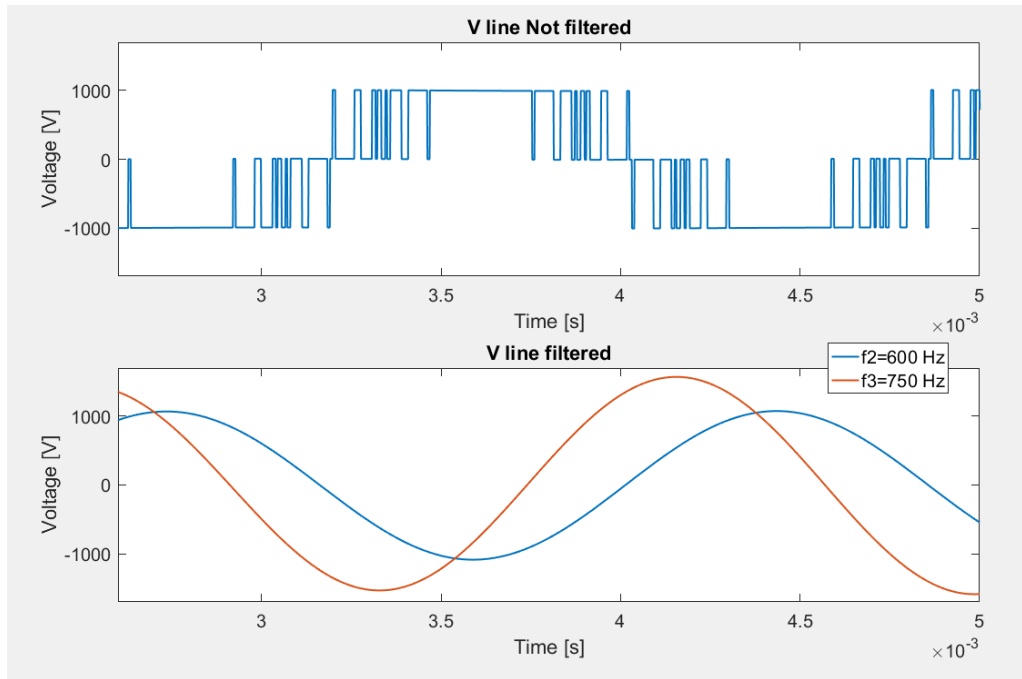
Fig 29. Line voltage (V$_{ab}$) with no filtration [upper], Line voltage (V$_{ab}$) with filtration [lower].

In the picture above only one line voltage is presented, the shape of both filtered and non-filtered voltages are accurate. One can see a different impact of applying a filter with different value of cut-off frequency. It seems that the optimal cut-off frequency for 2nd order low pass filter is around 750 kHz Output power is 85 %   (1.7 *MW*) of the initially designed value. Reactive power is equal to zero after filtration (meets the power factor requirement). In addition to that, a Fourier transform was performed on the not filtered voltage:

Fig 30. Fourier transform of the Line voltage (V$_{ab}$) with no filtration.

25

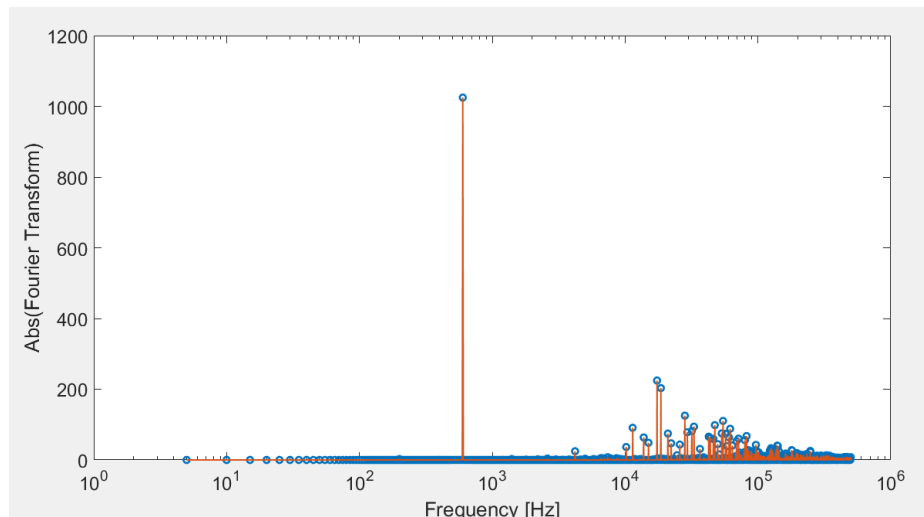It is clearly seen that the highest harmonic appear at 600 Hz and it's magnitude is bigger than for SPWM, all the other values are the undesired signal that should be filtered out. Total harmonic distortion factor was calculated using the same formula as for SPWM:

$$THD = \frac{\sqrt{\sum_{i>1} V_i^2}}{V_1} = 43{,}26\,\% \tag{3.9.}$$

The smaller value of THD means that filters dimensions could be smaller in reality comparing to e.g. SPWM modulation, however, more testing should be done in order to validate the results. The higher magnitude at 600 Hz harmonic proves higher step up capability of SHE modulation. Efficiency was calculated in the same way as in figure 23 in SPWM modulation.

Table 6. Calculation of energy for 294 cycles, filter f$_{cut-off}$ = 750 Hz.

	E$_{DC}$[W]	E$_{AC}$ [W]
SHE	838270.9	829507.5

$$\boldsymbol{Efficiency} = \frac{E_{in}}{E_{out}} = \frac{E_{AC}}{E_{DC}} = \frac{829507.5}{8838270.9} = 98.95\,\% \tag{3.10.}$$

Table 7. Features summary for SHE modulation, filter with f$_{cutoff}$ = 750 Hz.

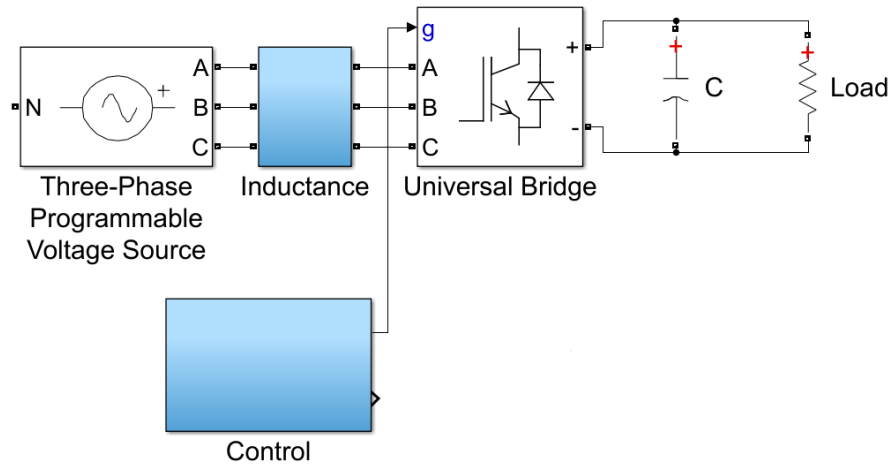| THD (V$_{not-filtered}$)	**Losses**	L	C	Power (ref to 2 MW)
43.26 %	**1.05 %**	2x159 uH	566 uF	85 %

1.4. Rectifier

Fig. 31. AC/DC converter, block diagram.

The AC/DC model consists of a three-phase AC source, universal bridge together with a control of the switches. In this case additionally set of inductances at input to the universal

bridge are needed, this block acts as a current stabilizer. Load resistance was chosen experimentally so that the DC voltage is equal to 1000 *V*.

3.4.1. DQ control

It was decided to use MOSFET switches and unipolar PWM control with the switching frequency 84 times higher than the frequency of the desired output signal.
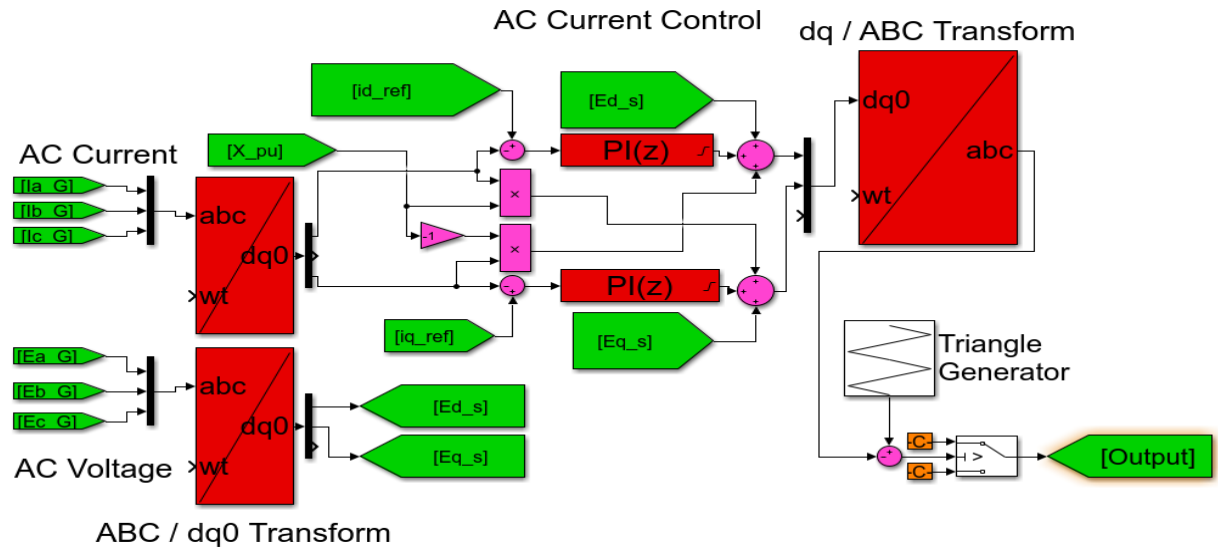
Fig 32. DQ control, block diagram.

	PI1	PI2
K_p	10	10
K_i	1	30
Limiter	1	2

Table 8. Gains of PI controllers

The control is based on Park transform together with PI blocks that control I_d and I_q currents. Finally the signals are transformed back to the 3-phase voltages, summed with a triangle signal and compared with 1. It is the most sophisticated part of the project. The gains were obtained experimentally, however it would be possible to linearize the circuit, find it's transfer function and tune PI controllers analytically.

27

Fig 33. Rotating frame [26].

$$\begin{bmatrix} u_d \\ u_q \\ u_0 \end{bmatrix} = \frac{2}{3} \begin{bmatrix} \cos(\omega t) & \cos(\omega t - \frac{2\pi}{3}) & \cos(\omega t + \frac{2\pi}{3}) \\ -\sin(\omega t 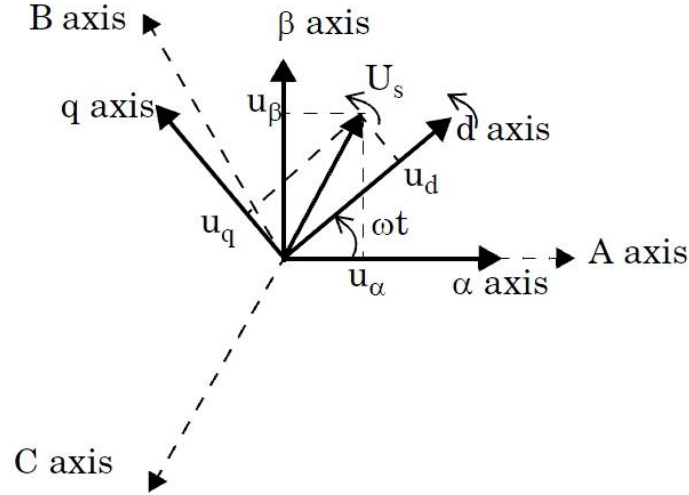- \frac{2\pi}{3}) & -\sin(\omega t - \frac{2\pi}{3}) & -\sin(\omega t - \frac{2\pi}{3}) \\ 1/2 & 1/2 & 1/2 \end{bmatrix} \begin{bmatrix} u_a \\ u_b \\ u_c \end{bmatrix}$$

Fig 34. Park's transformation from three-phase to rotating dq0 coordinate system [26].

The transformation to DQ rotating frame is necessary, because PID controllers can be used only for constant reference signals. Even though the I_q and I_d currents are demanded values, it is the voltage signal that is used to produce PWM modulation. For that reason the impedance X is multiplied by the I_q and I_d currents (XI=V). An adder adds the signal from PI controller, voltage across the impedance and the input voltage. Then the sum is converted back to ABC signals. At the end the signals are added to a triangle wave with operational frequency and compared to 1. The bigger is the error of I_d or I_q current, the higher amplitude ABC voltages will be, thus the higher the amplitude of ABC voltages. The longer the signal is greater than 1 and the longer a pair of switches will be switched on, diminishing the error.

1.4.1.1. Filter

Filter consist only of one capacitor on a DC side, connected to the load in parallel. The values of the inductance and capacitance are 155 mH and 20 µF.
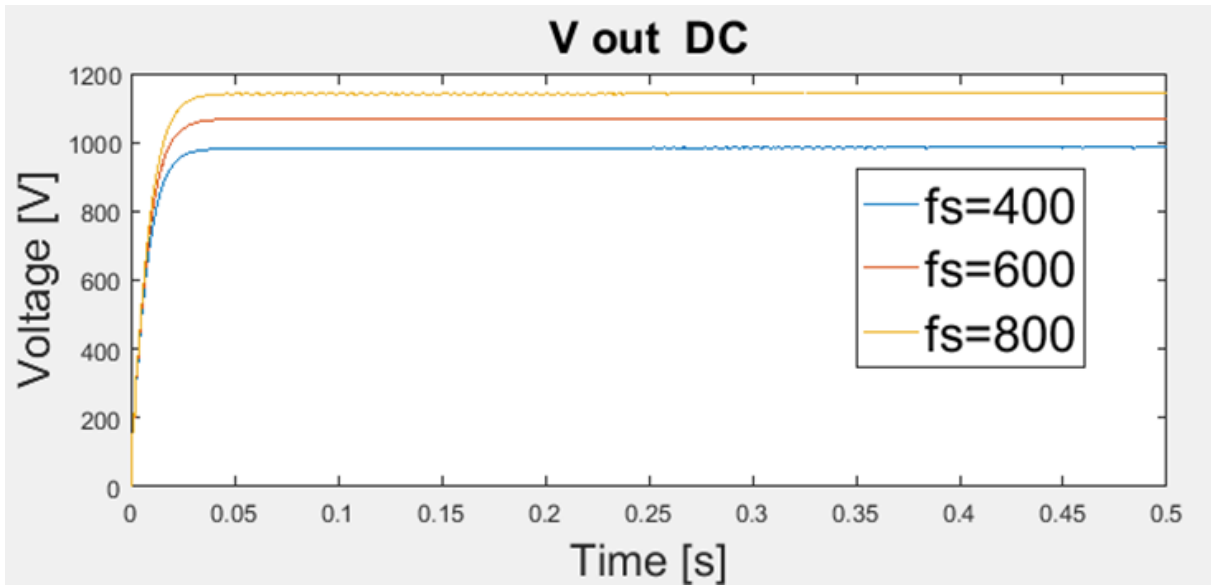
Fig 35. Output voltage, influence of operating frequency, R = 9 Ω.

On the plot, one can see the influence of the operating frequency on the DC voltage, for the same load condition and the PID tuning. A specific output voltage can be maintained for given operational frequency. Unfortunately the control is set to maintain I_q and I_d currents, not the output voltage.

Fig 36. Output voltage, influence of Load resistance, fs=600 Hz.

In addition to that, due to usage of high resistance (R = 9 Ω), the DC current drops to about 120 A in steady state, which means that the output power will be only 12 % (120 kW) of the

initially designed value. Reactive power is also significant (does not meet the power factor requirement). It means that, in the future the control has to be enhanced so that the voltage output is maintained for a re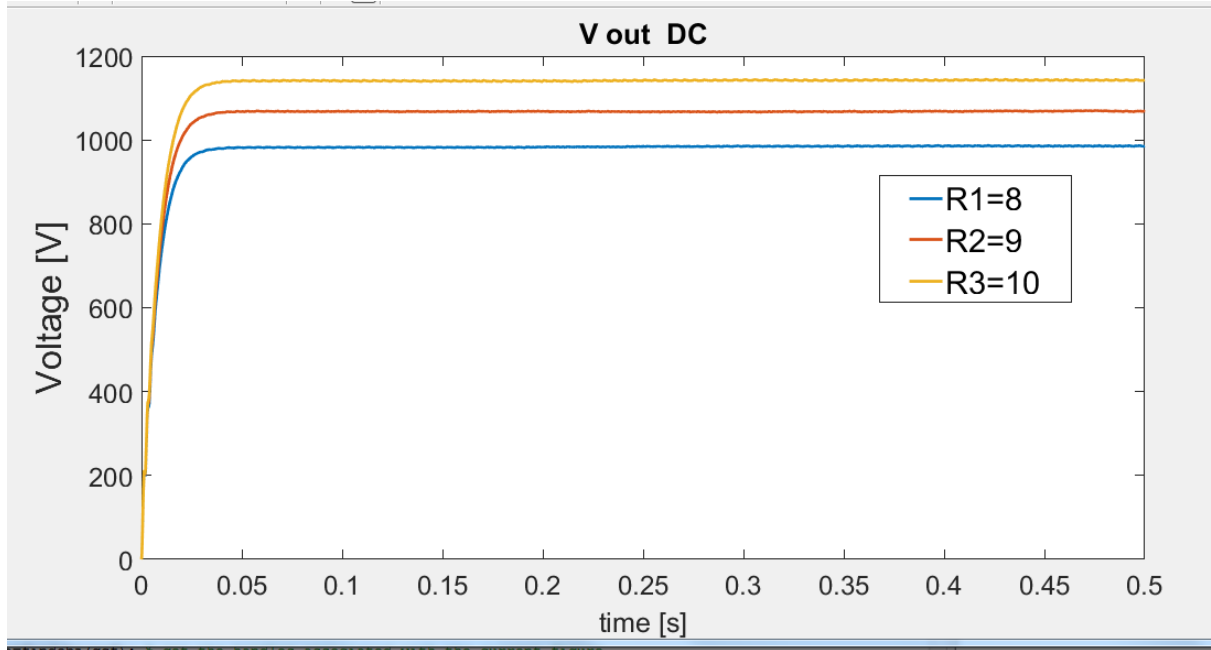alistic variable frequency of the inverter. That change has to be implemented to run the motor at desired rotational speed and to be able to provide sufficient output current.

In addition to that, a Fourier transform was performed on the input current, and THD was nearly equal to 0% which is a very good result. Efficiency was calculated in the same way as in figure 23 in SPWM modulation.

Table 9. Calculation of energy.

	E_{AC} [W]	E_{DC} [W]
DQ	57206	57025

$$Efficiency = \frac{E_{in}}{E_{out}} = \frac{E_{AC}}{E_{DC}} = \frac{57025}{57206} = 99,68\ \% \qquad (3.11.)$$

Unfortunately, due to significant power drop, the efficiency figure cannot be compared directly to other modulations that operate with the power close to initially designed value.

Table. 10. Parameters of the converters.

THD (input current)	**Losses**	L	C	Power (ref to 2 MW)
~ 0 %	**0.32 %**	1.55 mH	1 mF	12 %

3.4.2. Thyristor rectifier

Rectifier based on thyristors does not meet the project's requirement regarding the bi-directionality of the converter, however, it was used in order to compare it's features to other modulation (DQ control). Inductance and Capacitance were chosen experimentally to 0.1 mH, and 20 mF.

3.4.2.1.   Control

Traditional thyristor control was implemented based on **[28]**. The pulses were generated by matlab's pulse generator blocks.
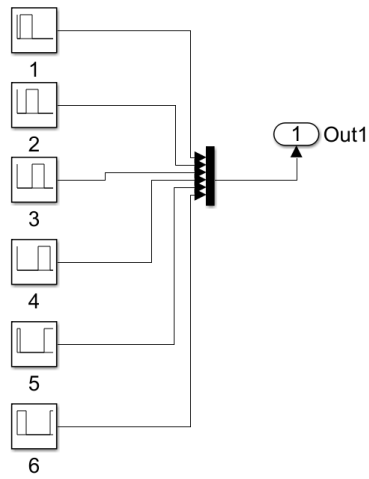
Fig. 37. Control, block diagram.

Fig. 38. Control

31
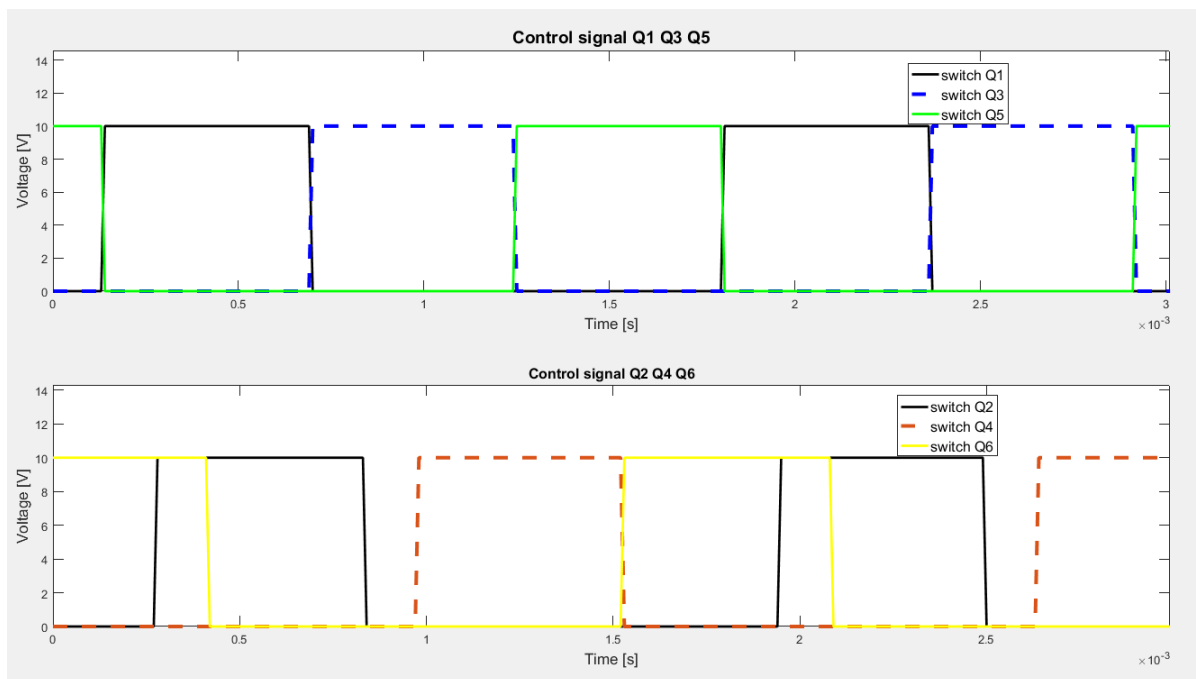
3.4.2.2. Results
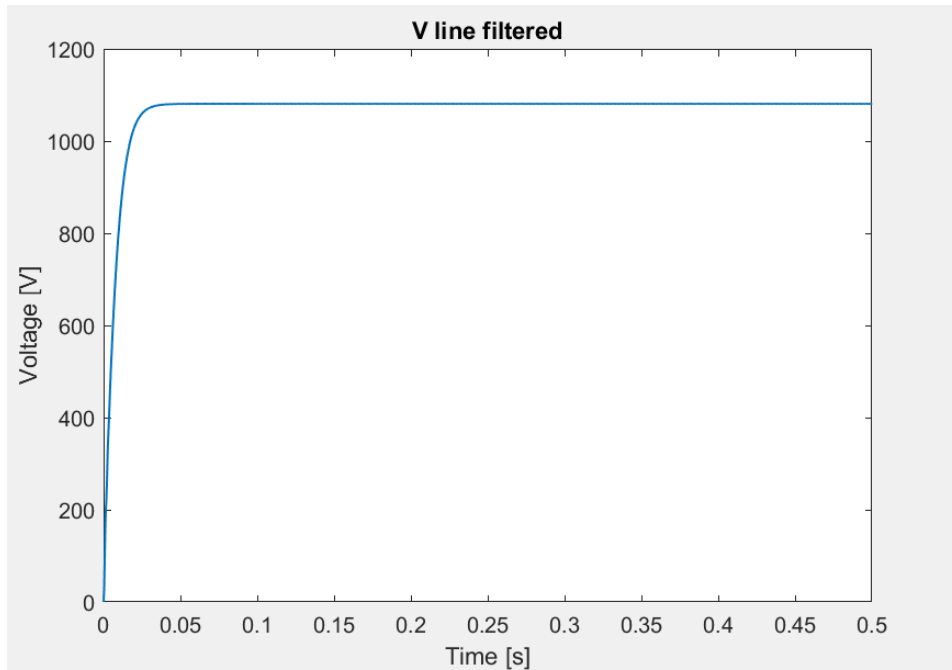
Fig. 39. Output voltage, R=0.7 Ω.

Efficiency was calculated in the same way as in figure 23 in SPWM modulation.

Table 11. Calculation of energy

	E_{AC} [W]	E_{DC} [W]
Thyristor	831166.7	784390.6

.

$$\boldsymbol{Efficiency} = \frac{E_{in}}{E_{out}} = \frac{E_{AC}}{E_{DC}} = \frac{831166.7}{784390.6} = 94.37\% \qquad \textbf{(3.12.)}$$

Table. 12. Parameters of the converters.

THD (input current)	Losses	L	C	Power (ref to 2 MW)
~ 0 %	5.63 %	0.1 mH	20 mF	86 %

DC current is equal to about 1600 *A* in steady state, which means that the output power will be only 86% (1.7 *MW*) of the initially designed value. Reactive power is also significant (does not meet the power factor requirement).

4. Control of induction motor

Additionally to the experiments presented above a model of a 3-phase induction model with a sensor control was introduced and its efficiency was calculated for different types of load. The simulation model is an enhanced version of the one provided by Matlab examples in 2017. Thanks to that, additional simulation it was possible to check the performance of a motor and its capability to maintain desired speed at different torque conditions, also in transient states.
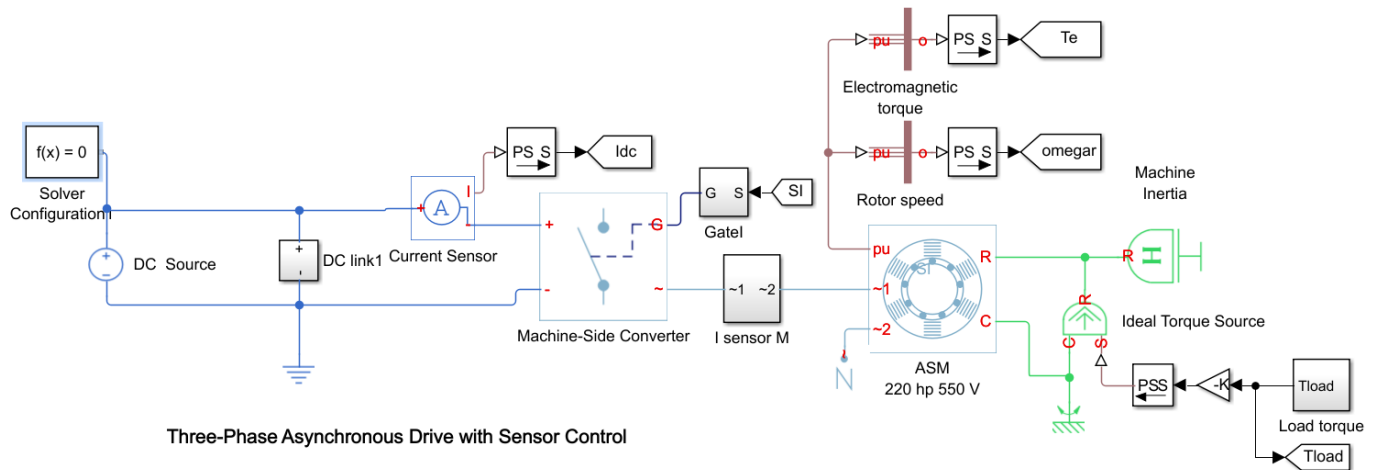

Figure 40. Additional model for induction machine control.

This block is very similar to the inverter block presented in *section 1.3 Inverter*, however the load is modeled as induction motor, described in section *2.11. Induction machine*. In this example SPWM and DQ control was used for the control. Vector control is used to enable DC machine-like controllability from an AC machine, An AC machine is not so simple because of the interactions between the stator and the rotor fields, whose orientations are not held at 90 degrees but vary with the operating conditions by orienting the stator current with respect to the rotor flux so as to attain independently controlled flux and torque.

$$V_{qs} = R_s i_{qs} + \frac{d\psi_{qs}}{dt} + \omega_e \psi_{ds} \qquad (4.1.)$$

$$V_{ds} = R_s i_{ds} + \frac{d\psi_{ds}}{dt} - \omega_e \psi_{qs} \qquad (4.2.)$$

$$0 = R_r i_{qr} + \frac{d\psi_{qr}}{dt} + (\omega_e - \omega_r)\psi_{dr} \qquad (4.3.)$$

$$0 = R_r i_{dr} + \frac{d\psi_{dr}}{dt} + (\omega_e - \omega_r)\psi_{qr} \qquad (4.4.)$$

$$T_e = 1.5p\frac{L_m}{L_r}(\psi_{dr}i_{qs} + \psi_{qr}i_{ds}), \text{ where} \tag{4.5.}$$

$$\psi_{qs} = L_s i_{qs} + L_m i_{qr}$$

$$\psi_{ds} = L_s i_{ds} + L_m i_{dr}$$

$$\psi_{qr} = L_r i_{qr} + L_m i_{qs}$$

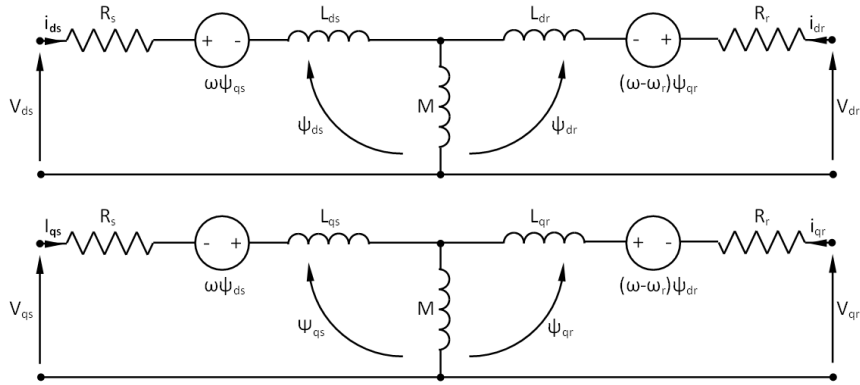$$\psi_{dr} = L_r i_{dr} + L_m i_{ds}$$

[30]

Figure 41. DQ induction machine model.

The objective is to de-couple the flux and torque producing components of the stator current This can be achieved if the rotor flux linkage space vector has constant amplitude and d-axis of the is aligned with synchronous rotating reference frame. This will mean that

$$\psi_{qr} = \frac{d\psi_{qr}}{dt} = \frac{d\psi_r}{dt} = 0 \text{ and } \psi_{qr} = \psi_r \tag{4.5.}$$

$$\omega_{sl} = (\omega_e - \omega_r) = \frac{L_m R_r}{\psi_r L_r}i_{qs} \tag{4.5.}$$

$$\boldsymbol{T_e = 1.5p\frac{L_m}{L_r}\psi_r i_{qs}} \tag{4.5.}$$

$$\frac{d\psi_r}{dt} = -\frac{R_r}{L_r}\psi_r + \frac{L_m R_r}{L_r}i_{ds} \tag{4.5.}$$

These expressions show that the d-axis component of the stator current controls rotor flux, and the q-axis component of the current controls slip and, therefore, torque. The electric torque is proportional to the i_{qs} component and the relation between the flux φ_r is described by a first-order linear transfer function with a time constant L_r / R_r **[29]**.
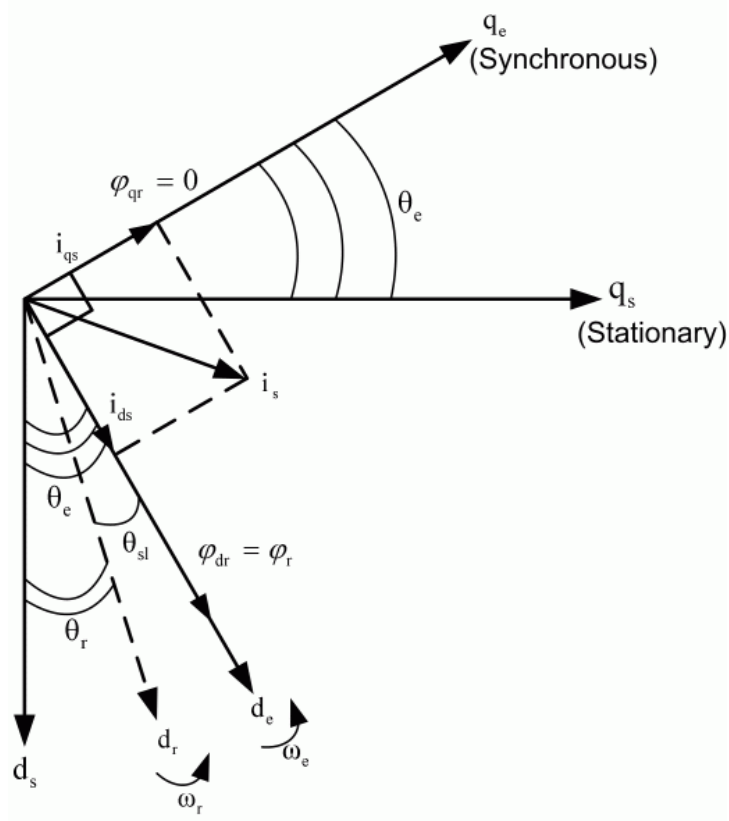
Figure 42. Rotor Flux Position Obtained from the Slip and Rotor Positions.
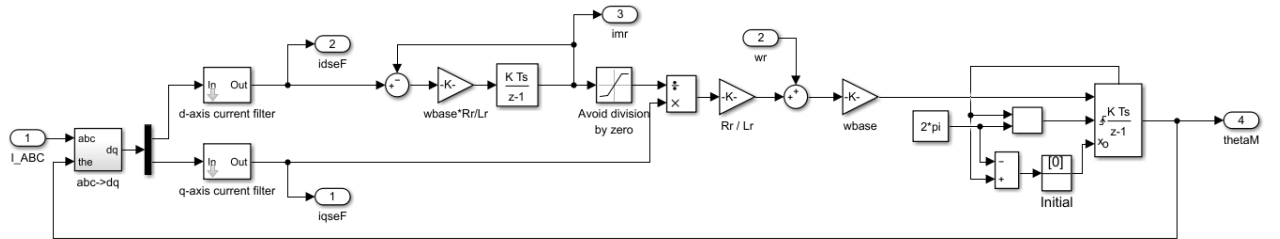
Figure 43. Flux Observer.

Flux observing block is transforming between the rotating 3-phase and rotating 2-phase (dq), integration d axis current, then using the equations described above slip speed is obtained and added to the measured speed. Thanks to that the rotational speed of the flux is observed and switching signal thetaM can be calculated and then used for switching the full bridge converter with appropriate frequency rate.
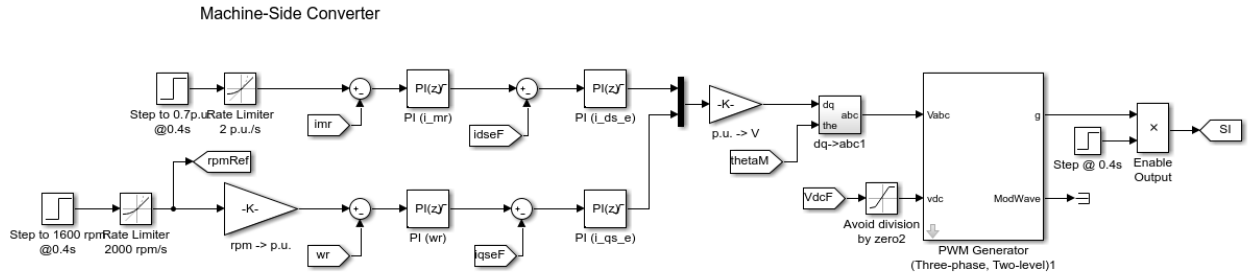
Figure 44. Machine-side converter control.

The block is a full control of the machine that sets reference speed of its rotation and level of magnetization of parallel branch. PIs tuning were not part of the project and were taken directly from the MATLAB example. PWM generator is exactly the same as the one described in section *1.3.2.1. control*.

Figure 45. Performance of the induction machine, under different load condition.

36
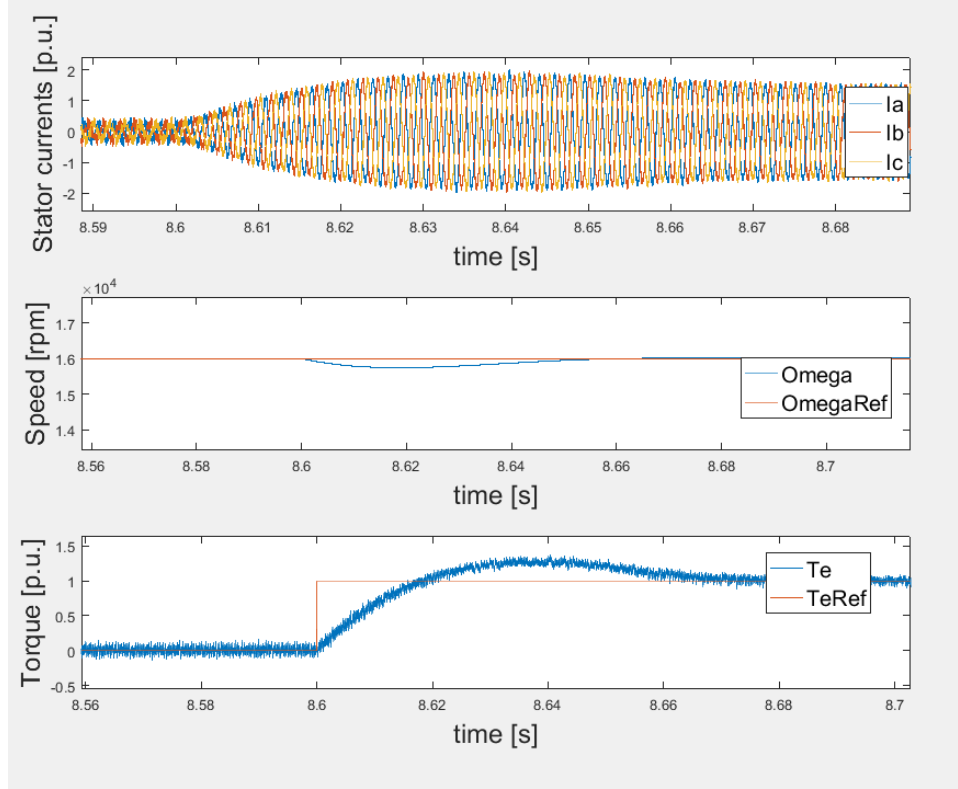
Figure 46. Performance of the induction machine, zoomed for the transient change of load.

Simulations show speeding up of the induction machine from 0 *rpm* to its rated speed of 16000 *rpm* in 8 *seconds* with no external torque, then it is subjected to the various torq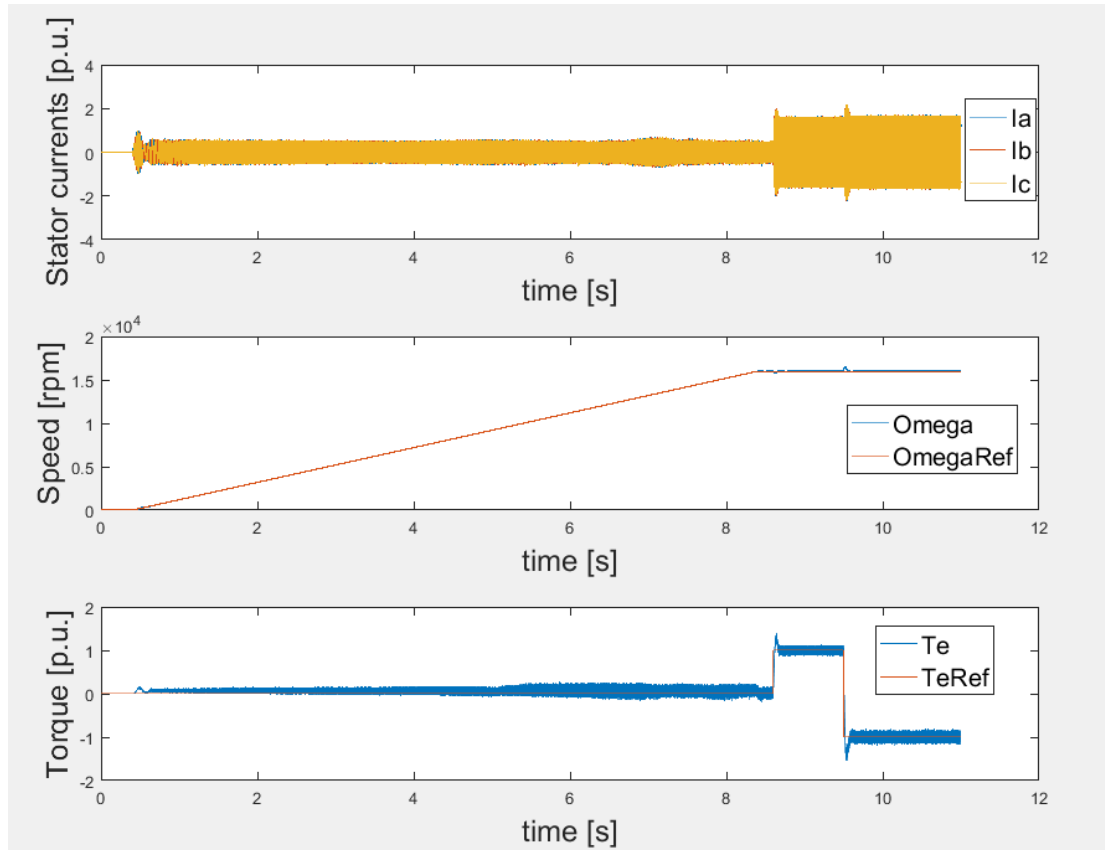ue conditions of 1 *p.u.* and -1 *p.u.* Simulations confirm the possibility of the control induction motor under various torque conditions. The changes of the torque are seen at instances of 8.6 *s* and 9 *s* and in spite of small changes of the rotor speed, machine manages to maintain its speed at 16 000 *rpm* which is a corresponding to 600 *Hz* for a 2 pole motor (detailed parameters of the machine are attached in the appendix). One can observe how stator currents are changing their magnitude at the time of transients. Positive torque means that the machine is additionally loaded, whereas negative torque means that the machine acts as a generator.

The additional test shows that the induction machine with parameters described in the objectives can be in fact controlled, both in steady state and in transients, no matter what the torque condition is. Efficiency of the power converter was calculated in the same manner as described in the sections above for various torque conditions and presented in a table below. The results were obtained only for steady state speed (transients are neglected)

Table 14. Efficiency of the induction machine under various torque conditions..

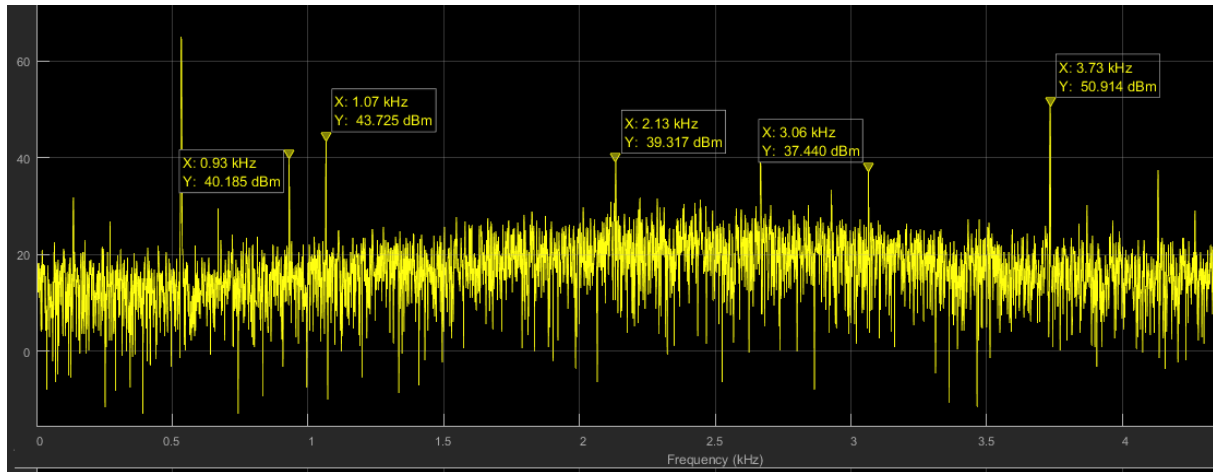| Torque [p.u.]	Input Power [W]	Output Power [W]	Efficiency	Loss [%]
T=0	991113.7	972375.0	0.9811	1,89
T=0.5	6865094	6823602.8	0.994	0,6
T=1	13099752	13005329.8	0.9928	0,72
T=-1	-9648904.6	-9741071.9	0.9905	0,95
T=-0.5	-4512362.2	-4552547	0.9912	0,88

Fig 48. Harmonics of the Ia stator current for torque equals to zero.

The efficiency seems to be worst when the speed has to be maintained at no torque. Efficiency is also worse when the machine works as a generator than as a motor. Fourier transform was performed on the A phase of the current, yet not deeply analyzed and compared with different torque conditions.

5. Summary

Most of the project success criteria were achieved. Two models of the three phase rectifier and the three phase inverter were designed and simulated. Various modulation techniques were tested together with other system parameters like: filters cut-off frequency and operating frequency.

Table 15. Parameters of the converters.

	Modulation Technique	THD ($V_{notfiltered}$/ I_{input})	**Losses**	L	C	Power (ref to 2 MW)
Inverter	SPWM	60,95 %	**1.11 %**	2x 159 uH	166 uF	60 %
Inverter	SHE	43,26 %	**1.05 %**	2x 159 uH	166 uF	85 %
Rectifier	Thyristor	~ 0 %	**5.63 %**	0.1 mH	20 mF	86 %
Rectifier	DQ control	~ 0 %	**0.317 %**	1.55 mH	1 mF	12 %

Two modulation techniques for the inverter gives very comparable results. SHE seems to be better in every single aspect. THD of not filtered voltage is smaller, hence smaller filters could be possibly used. It is more efficient, has greater power and step-up capability. Nonetheless, switching frequency of SPWM is only 10 times higher than the operational frequency, resulting in 6 kHz switching. It is known that IGBT could operate on much higher frequency, therefore the results may be different if the converter was run on higher frequency. On the other hand, an increase of switching frequency for SHE modulation would require solving the set of equations eliminating higher number of harmonics which is a difficult task.

Rectifier with DQ control is able to output correct DC voltage (1000V), but it does not meet other design requirements: nominal power, power factor. It is also hard to compare it to the traditional rectifier based on thyristors due to the significant power mismatch.

In spite of not meeting the design requirements, the best converters have small losses (less than 2%), however, that figure for a system of 2 MVA would mean about 40 kW of power that will be dissipated in the form of heat.

Additionally another simulation was done that tested the performance of the load modelled as an induction machine. It showed that control and maintaining desired speed is possible and its efficiency was calculated paving the way for the future modelling of entire system.

6. Future work

Due to the fact that there are so many issues that should be investigated, only part of the phenomena and parameters were checked. There is still room for improvement and project extenstion, those are the proposals:

- Designing EMI filter and adequate cooling system and estimating volume and weight of the entire system.
- Ensuring that the converter provide the power stated in the design requirements and that the standard's power factor is respected.
- Modelling generator
- Estimation of transmission losses.
- Enhancing modulation technique for rectifier that would maintain the DC voltage no matter what the operational frequency is.
- Connecting rectifier and inverter together and analyzing the system performance.
- Analyzing the influence of other parameters on the system performance like:
  Type of switches (e.g. MOSFET), operational frequency for inverter, switching frequency.
- Testing more topologies e.g. Vienna rectifier or Autotransformer rectifier unit.

References

[1] Action Plan for Energy Efficiency (2007-12), *Eur-lex.europa.eu*, 2016. [Online]. Available:

http://eur-lex.europa.eu/legal-

content/EN/TXT/HTML/?uri=URISERV:l27064&from=EN.

[Accessed: 08- Oct- 2016].

[2] Dr P. Janger Arnold, *Seminar on High Power/Medium*

Voltage Propulsion Network for Electro/Hybrid Aircraft, Ottobrunn, 2016.

[3] Mohan, N., Undeland, T. M., & Robbins, W. P. (1995). Power electronics: Converters, applications, and design. New York: Wiley.

[4] Ł. Strzak, *Wprowadzenie do elektroniki mocy Elektroniczne układy przekształtnikowe Przyrządy półprzewodnikowe mocy*, 2015. [Online]. Available:

http://neo.dmcs.p.lodz.pl/pium/instrukcje/pium_0_1-6-0.pdf.

[Accessed: 08- Oct- 2016].

[5] Intechopen.com, 2016. [Online].

Available: http://www.intechopen.com/source/html/43396/media/image16_w.jpg.

[Accessed: 28- Nov- 2016].

[6] Lh5.ggpht.com, 2016. [Online]. Available: http://lh5.ggpht.com/-

SsEQOKFMHxE/T2SewvKGaqI/AAAAAAAAEoM/5Q2buwEb630/image_thumb%

25255B11%25255D.png?imgmax=800. [Accessed: 28- Nov- 2016].

[7] W. Storr, *Second Order Filter | Second Order Low Pass Filter Design*, Basic Electronics Tutorials, 2013. [Online]. Available: http://www.electronics-tutorials.ws/filter/second-order-filters.html. [Accessed: 06- Dec- 2015].

[8] R. Mancini and T. Kugelstadt, *Op Amps For Everyone*, Chapter 16 Active Filter Design Techniques, Sep. 2001.

[9] 2016. [Online]. Available: https://www.techopedia.com/definition/9034/pulse-width-modulation-pwm. [Accessed: 28- Nov- 2016].

[10] 2016. [Online]. Available: https://www.quora.com/What-should-be-cared-for-when-choosing-bipolar-or-unipolar-voltage-control-circuits-for-switching-PWM-frequency-in-inverters. [Accessed: 28- Nov- 2016

[11] J. Fraile, Energy systems, Topic *Electrónica de Potencia Parte VI. Inversores*, class lecture, Technical University of Madrid, summer semester 2014/2015.

[12] "More Electric Aircraft - MEA - Next Generation Aircraft Power", Moreelectricaircraft.com, 2016. [Online]. Available: http://www.moreelectricaircraft.com/. [Accessed: 28- Nov- 2016].

[13] 2016. [Online]. Available: http://www.radio-electronics.com/info/rf-technology-design/rf-filters/simple-lc-lowpass-filter-design.php. [Accessed: 28- Nov- 2016].

[14] *K. Rajashekara, More Electric Aircraft Trends [Technology Leaders*], IEEE Electrification Magazine, vol. 2, no. 4, pp. 4-39, 2014.

[15] P.M.1 Peeters, J.Middel, A. Hoolhorst, *Fuel efficiency of commercial aircraft Fuel efficiency of commercial aircraft An overview of historical and future trends*, 2015.

[16] Kamiar J. Karimi, *Future Aircraft Power Systems- Integration Challenges*, 2007.

[17] A. Kharina, D. Rutherford, *Fuel efficiency trends for new commercial jet aircraft: 1960 to 2014*, 2015.

[18] 2017. [Online]. Available: http://www.srmuniv.ac.in/sites/default/files/downloads/unit_2_eee_pg.pdf. [Accessed: 25- Mar- 2017].

[19] M. Hartmann*, Ultra-Compact and Ultra-Efficient Three-Phase PWM Rectifier Systems for More Electric Aircraft,* Ph.D. dissertation, ETH Zurich, 2011.

[20] RTCA Inc., *Enviromental Conditions and Test Procedures for Airborne Equipment - RTCA DO-160F*, RTCA Inc. Std.

[21] MIL-STD-704F, *Aircraft Electric Power Characteristics*, Department of Defense Std., March 12, 2004.

[22] C. R. Avery, S. G. Burrow, and P. H. Mellor, "Electrical Generation and Distribution for the More Electric Aircraft," in *Proc. Of the 42nd Int. Universities Power Engineering Conf. (UPEC '07)*, 2007, pp. 1007–1012

[23] M. E. Elbuluk and M. D. Kankam, "Potential Starter/Generator Technologies for Future Aerospace Applications," *IEEE Aerospace and Electronic Systems Magazine*, vol. 12, no. 5, pp. 24–31, 1997.

[24]   T. Friedli and J. W. Kolar, "Comprehensive Comparison of ThreePhase AC-AC Matrix Converter and Voltage DC-Link Back-toBack Converter Systems," in *Proc. of the Int. Power Electronics Conf. (IPEC '10)*, 2010, pp. 2789–2798

[25]   2017. [Online]. Available: https://uk.mathworks.com/help/physmod/sps/powersys/ref/pwmgenerator.html. [Accessed: 30- Mar- 2017].

[26]   2017. [Online]. Available: https://uk.mathworks.com/help/physmod/sps/powersys/ref/abctodq0dq0toabc.html. [Accessed: 30- Mar- 2017].

[27]   D. Ahmadi, K. Zou, C. Li, Y. Huang and J. Wang, "A Universal Selective Harmonic Elimination Method for High-Power Inverters," in *IEEE Transactions on Power Electronics*, vol. 26, no. 10, pp. 2743-2752, Oct. 2011. doi: 10.1109/TPEL.2011.2116042

[28]   "OPERATION OF A 3-PHASE FULLY-CONTROLLED RECTIFIER", *Technik-emden.de*, 2017. [Online]. Available: http://www.technik-emden.de/~elmalab/projekte/ws9899/pe_html/ch05s1/ch05s1p1.htm. [Accessed: 30- Mar- 2017].

[29]   *D. Motor and S. Motor, "Model induction motor powered by ideal AC supply - MATLAB - MathWorks United Kingdom", Uk.mathworks.com, 2017. [Online]. Available: https://uk.mathworks.com/help/physmod/elec/ref/inductionmotor.html. [Accessed: 04- Sep- 2017]*

[30]   *Simulate an AC Motor Drive - MATLAB & Simulink - MathWorks United Kingdom", Uk.mathworks.com, 2017. [Online]. Available: https://uk.mathworks.com/help/physmod/sps/powersys/ug/simulating-an-ac-motor-drive.html. [Accessed: 06- Sep- 2017].*

APPENDIX

```
m=1;

f1 = @(x1, x2, x3, x4, x5, x6, x7) -1+2*cos(x1)-2*cos(x2)+2*cos(x3)-
2*cos(x4)+2*cos(x5)-2*cos(x6)+2*cos(x7)-m(k)*pi/4;

f2 = @(x1, x2, x3, x4, x5, x6, x7) -1+2*cos(15*x1)-2*cos(15*x2)+2*cos(15*x3)-
2*cos(15*x4)+2*cos(15*x5)-2*cos(15*x6)+2*cos(15*x7)

f3 = @(x1, x2, x3, x4, x5, x6, x7) -1+2*cos(5*x1)-2*cos(5*x2)+2*cos(5*x3)-
2*cos(5*x4)+2*cos(5*x5)-2*cos(5*x6)+2*cos(5*x7)

f4 = @(x1, x2, x3, x4, x5, x6, x7) -1+2*cos(7*x1)-2*cos(7*x2)+2*cos(7*x3)-
2*cos(7*x4)+2*cos(7*x5)-2*cos(7*x6)+2*cos(5*x7)

f5 = @(x1, x2, x3, x4, x5, x6, x7) -1+2*cos(9*x1)-2*cos(9*x2)+2*cos(9*x3)-
2*cos(9*x4)+2*cos(9*x5)-2*cos(9*x6)+2*cos(9*x7)

f6 = @(x1, x2, x3, x4, x5, x6, x7) -1+2*cos(11*x1)-2*cos(11*x2)+2*cos(11*x3)-
2*cos(11*x4)+2*cos(11*x5)-2*cos(11*x6)+2*cos(11*x7)

f7 = @(x1, x2, x3, x4, x5, x6, x7) -1+2*cos(13*x1)-2*cos(13*x2)+2*cos(13*x3)-
2*cos(13*x4)+2*cos(13*x5)-2*cos(13*x6)+2*cos(13*x7)

x0 = [0.01,0.01,0.1,0.02,0.4,0.4,0.6]; % initial guess

fun = @(x) [f1(x(1),x(2),x(3),x(4),x(5),x(6),x(7)),
f2(x(1),x(2),x(3),x(4),x(5),x(6),x(7)),
f3(x(1),x(2),x(3),x(4),x(5),x(6),x(7)),
f4(x(1),x(2),x(3),x(4),x(5),x(6),x(7)),f5(x(1),x(2),x(3),x(4),x(5),x(6),
x(7)),f6(x(1),x(2),x(3),x(4),x(5),x(6),x(7)),f7(x(1),x(2),x(3),x(4),x(5)
,x(6),x(7))];
lb = [0,0,0,0,0,0,0]; %Solutions from 0 to pi/4
ub = [0.1,0.3,0.785,0.785,0.785,0.785,0.785];

options = optimoptions('lsqnonlin','Display','iter','TolX',1e-5);
x = lsqnonlin(fun,x0,lb,ub,options);
```

Fig 1. Code, N=3, 5 and 7 eliminated, m=1.

```
%% Induction machine parameters
Pn  = 2e6;       % W, nominal power
Vn  = 1000;          % V,  rms phase-to-phase, rated voltage
fn  = 600;           % Hz, rated frequency 60


Rs  = 0.0139;    % pu, stator resistance
Lls = 0.0672;    % pu, stator leakage inductance
Rr  = 0.0112;    % pu, rotor resistance, referred to the stator side
Llr = 0.0672;    % pu, rotor leakage inductance, referred to the stator side
Lm  = 2.717;     % pu, magnetizing inductance
Lr = Llr+Lm;     % pu, rotor inductance
Ls = Lls+Lm;     % pu, stator inductance


H = 0.2734;  % s, moment of inertia
F = 0.0106;  % pu,friction coefficient
p = 2;          % pole pairs


Vbase = Vn/sqrt(3)*sqrt(2);   % V, base voltage, peak, line-to-neutral 408
Ibase = Pn/(1.5*Vbase);   % A, base current, peak 3267
Zbase = Vbase/Ibase;      % ohm, base resistance 0.124
wbase = 2*pi*fn;              % rad/s, base elec. radial frequency
Tbase = Pn/(wbase/p);     % N*m, base torque


Rss = Rs*Zbase;  % ohm, stator resistance
Xls = Lls*Zbase; % ohm, stator leakage reactance
Rrr = Rr*Zbase;  % ohm, rotor resistance, referred to the stator side
Xlr = Llr*Zbase; % ohm, rotor leakage reactance, referred to the stator side
Xm = Lm*Zbase;   % ohm, magnetizing reactance
```

Fig. 2. Parameters of the induction machine, grid side converter and control.

```
%% Control parameters
Ts = 5e-6;          % s, fundamental sample time
fsw = 2e4;          % Hz, switching frequency
Tsc = 1/(fsw*10); % s, control sample time

% Machine-side PI parameters
Kp_ids = 1.08;
Ki_ids = 207.58;
Kp_imr = 52.22;
Ki_imr = 2790.51;
Kp_iqs = 1.08;
Ki_iqs = 210.02;
```

Fig. 3. Control and machine side converter parameters.

OŚWIADCZENIE

Daniel Dobiński
(Imię i nazwisko studenta)

ul. Anny Jagiellonki 2/37, Łódź 92-414
(Adres)

171078
(Nr albumu)

Wydział EEIA
……………………………………………………….
(Jednostka organizacyjna prowadząca studia)

elektronika i telekomunikacja
……………………………………………………….
(Kierunek studiów)

studia II stopnia, stacjonarne
……………………………………………………….
(Poziom kształcenia i forma studiów)

Oświadczam, że poinformowano mnie o zasadach dotyczących kontroli oryginalności pracy dyplomowej w systemie antyplagiatowym.

Wyrażam zgodę na przetwarzanie*⁾ mojej pracy dyplomowej, a także na przechowywanie jej w celu realizowania procedury antyplagiatowej w bazie danych systemu antyplagiatowego.

……………………….......
(Podpis studenta)

……………, dn. ......………………

OŚWIADCZENIE

o samodzielności wykonania i oryginalności pracy dyplomowej

Daniel Dobiński
(Imię i nazwisko studenta)

ul. Anny Jagiellonki 2/37, Łódź 92-414
(Adres)

208253
(Nr albumu)

Wydział EEIA
…………………………………………………………
(Jednostka organizacyjna prowadząca studia)

elektronika i telekomunikacja
…………………………………………………………
(Kierunek studiów)

studia I stopnia, stacjonarne
…………………………………………………………
(Poziom kształcenia i forma studiów)

Świadomy/a odpowiedzialności karnej za składanie fałszywych zeznań oświadczam, że przedkładana praca dyplomowa inżynierska *⁾ na temat: Badania technologii elektronicznych

---

przetwornic mocy w celu poprawy osiągów w układach elektrycznych samolotów przyszłości, została wykonana przeze mnie samodzielnie.

Jednocześnie oświadczam, że ww. praca:

- nie narusza praw autorskich w rozumieniu ustawy z dnia 4 lutego 1994 r. o prawie autorskim i prawach pokrewnych (t.j. Dz. U. z 2006 r. Nr 90, poz. 631, z późn. zm.) oraz dóbr osobistych chronionych prawem cywilnym, a także nie zawiera danych i informacji, które uzyskałem/am w sposób niedozwolony,

- nie była wcześniej podstawą żadnej innej urzędowej procedury związanej z nadawaniem dyplomów wyższej uczelni lub tytułów zawodowych.

………………………….......
(Podpis studenta)

…………., dn. ......…………………

OŚWIADCZENIE

o zgodności wersji elektronicznej pracy dyplomowej

z przedstawionym wydrukiem komputerowym

Daniel Dobiński
(Imię i nazwisko studenta)

ul. Anny Jagiellonki 2/37, Łódź 92-414
(Adres)

208253
(Nr albumu)

Wydział EEIA
…………………………………………………………..
(Jednostka organizacyjna prowadząca studia)

elektronika i telekomunikacja
…………………………………………………………..
(Kierunek studiów)

studia II stopnia, stacjonarne
…………………………………………………………..
(Poziom kształcenia i forma studiów)

---

*) Wpisać odpowiednio: inżynierska, magisterska.

Świadomy odpowiedzialności karnej za składanie fałszywych zeznań oświadczam, że przedkładana na nośniku elektronicznym praca dyplomowa magisterska *⁾ na temat: Badania technologii elektronicznych przetwornic mocy w celu poprawy osiągów w układach elektrycznych samolotów przyszłości,

zawiera te same treści, co oceniany przez promotora i recenzenta wydruk komputerowy.

Jednocześnie oświadczam, że jest mi znany przepis art. 233 § 1 Kodeksu karnego określający odpowiedzialność za składanie fałszywych zeznań.

………………………….......
(Podpis studenta)

…..……….., dn ………..……… r.

……………………………………………………….
(Imię i nazwisko studenta)